

Determining the Dirac CP Violation Phase in the Neutrino Mixing Matrix from Sum Rules

I. Girardi^{a)}, S. T. Petcov^{a,b)} ¹ and A. V. Titov^{a)}

^a *SISSA/INFN, Via Bonomea 265, 34136 Trieste, Italy*

^b *Kavli IPMU (WPI), University of Tokyo, 5-1-5 Kashiwanoha, 277-8583 Kashiwa, Japan*

Abstract

Using the fact that the neutrino mixing matrix $U = U_e^\dagger U_\nu$, where U_e and U_ν result from the diagonalisation of the charged lepton and neutrino mass matrices, we analyse the sum rules which the Dirac phase δ present in U satisfies when U_ν has a form dictated by flavour symmetries and U_e has a “minimal” form (in terms of angles and phases it contains) that can provide the requisite corrections to U_ν , so that reactor, atmospheric and solar neutrino mixing angles θ_{13} , θ_{23} and θ_{12} have values compatible with the current data. The following symmetry forms are considered: i) tri-bimaximal (TBM), ii) bimaximal (BM) (or corresponding to the conservation of the lepton charge $L' = L_e - L_\mu - L_\tau$ (LC)), iii) golden ratio type A (GRA), iv) golden ratio type B (GRB), and v) hexagonal (HG). We investigate the predictions for δ in the cases of TBM, BM (LC), GRA, GRB and HG forms using the exact and the leading order sum rules for $\cos \delta$ proposed in the literature, taking into account also the uncertainties in the measured values of $\sin^2 \theta_{12}$, $\sin^2 \theta_{23}$ and $\sin^2 \theta_{13}$. This allows us, in particular, to assess the accuracy of the predictions for $\cos \delta$ based on the leading order sum rules and its dependence on the values of the indicated neutrino mixing parameters when the latter are varied in their respective 3σ experimentally allowed ranges.

Key words: neutrino physics, leptonic CP violation, sum rules.

¹Also at: Institute of Nuclear Research and Nuclear Energy, Bulgarian Academy of Sciences, 1784 Sofia, Bulgaria.

1 Introduction

One of the major goals of the future experimental studies in neutrino physics is the searches for CP violation (CPV) effects in neutrino oscillations (see, e.g., [1, 2]). It is part of a more general and ambitious program of research aiming to determine the status of the CP symmetry in the lepton sector.

In the case of the reference 3-neutrino mixing scheme¹, CPV effects in the flavour neutrino oscillations, i.e., a difference between the probabilities of $\nu_l \rightarrow \nu_{l'}$ and $\bar{\nu}_l \rightarrow \bar{\nu}_{l'}$ oscillations in vacuum [3, 4], $P(\nu_l \rightarrow \nu_{l'})$ and $P(\bar{\nu}_l \rightarrow \bar{\nu}_{l'})$, $l \neq l' = e, \mu, \tau$, can be caused, as is well known, by the Dirac phase present in the Pontecorvo, Maki, Nakagawa and Sakata (PMNS) neutrino mixing matrix $U_{\text{PMNS}} \equiv U$. If the neutrinos with definite masses ν_i , $i = 1, 2, 3$, are Majorana particles, the 3-neutrino mixing matrix contains two additional Majorana CPV phases [4]. However, the flavour neutrino oscillation probabilities $P(\nu_l \rightarrow \nu_{l'})$ and $P(\bar{\nu}_l \rightarrow \bar{\nu}_{l'})$, $l, l' = e, \mu, \tau$, do not depend on the Majorana phases² [4, 8]. Our interest in the CPV phases present in the neutrino mixing matrix is stimulated also by the intriguing possibility that the Dirac phase and/or the Majorana phases in U_{PMNS} can provide the CP violation necessary for the generation of the observed baryon asymmetry of the Universe [9, 10].

In the standard parametrisation [1] of the PMNS matrix we are going to employ in our further discussion, U_{PMNS} is expressed in terms of the solar, atmospheric and reactor neutrino mixing angles θ_{12} , θ_{23} and θ_{13} , respectively, and the Dirac and Majorana CPV phases, as follows:

$$U = VQ, \quad Q = \text{diag}(1, e^{i\frac{\alpha_{21}}{2}}, e^{i\frac{\alpha_{31}}{2}}), \quad (1)$$

where $\alpha_{21,31}$ are the two Majorana CPV phases and V is a CKM-like matrix,

$$V = \begin{pmatrix} c_{12}c_{13} & s_{12}c_{13} & s_{13}e^{-i\delta} \\ -s_{12}c_{23} - c_{12}s_{23}s_{13}e^{i\delta} & c_{12}c_{23} - s_{12}s_{23}s_{13}e^{i\delta} & s_{23}c_{13} \\ s_{12}s_{23} - c_{12}c_{23}s_{13}e^{i\delta} & -c_{12}s_{23} - s_{12}c_{23}s_{13}e^{i\delta} & c_{23}c_{13} \end{pmatrix}. \quad (2)$$

In eq. (2), δ is the Dirac CPV phase, $0 \leq \delta \leq 2\pi$, we have used the standard notation $c_{ij} = \cos \theta_{ij}$, $s_{ij} = \sin \theta_{ij}$, and $0 \leq \theta_{ij} \leq \pi/2$. If CP invariance holds, we have $\delta = 0, \pi, 2\pi$, the values 0 and 2π being physically indistinguishable.

The existing neutrino oscillation data allow us to determine the neutrino mixing parameters $\sin^2 \theta_{12}$, $\sin^2 \theta_{23}$ and $\sin^2 \theta_{13}$, which are relevant for our further analysis, with a relatively good precision [11, 12]. The best fit values and the 3σ allowed ranges of $\sin^2 \theta_{12}$, $\sin^2 \theta_{23}$ and $\sin^2 \theta_{13}$, found in the global analysis in ref. [11] read:

$$(\sin^2 \theta_{12})_{\text{BF}} = 0.308, \quad 0.259 \leq \sin^2 \theta_{12} \leq 0.359, \quad (3)$$

$$(\sin^2 \theta_{23})_{\text{BF}} = 0.437 (0.455), \quad 0.374(0.380) \leq \sin^2 \theta_{23} \leq 0.626(0.641), \quad (4)$$

$$(\sin^2 \theta_{13})_{\text{BF}} = 0.0234 (0.0240), \quad 0.0176(0.0178) \leq \sin^2 \theta_{13} \leq 0.0295(0.0298), \quad (5)$$

¹All compelling data on neutrino masses, mixing and oscillations are compatible with the existence of mixing of three light neutrinos ν_i , $i = 1, 2, 3$, with masses $m_i \lesssim 1$ eV in the weak charged lepton current (see, e.g., [1]).

²The Majorana phases can play important role, e.g., in $|\Delta L| = 2$ processes like neutrinoless double beta $((\beta\beta)_{0\nu^-})$ decay $(A, Z) \rightarrow (A, Z+2) + e^- + e^-$, L being the total lepton charge, in which the Majorana nature of massive neutrinos ν_i , if any, manifests itself (see, e.g., [5-7]).

where the values (values in brackets) correspond to neutrino mass spectrum with normal ordering (inverted ordering) (see, e.g., [1]), denoted further as NO (IO) spectrum.

In the present article we will be concerned with the predictions for the Dirac phase δ and will not discuss the Majorana phases in what follows. More specifically, we will be interested in the predictions for the Dirac CPV phase δ which are based on the so-called ‘‘sum rules’’ [13–15] (see also, e.g., [16–19]). The sum rules of interest appear in an approach aiming at quantitative understanding of the pattern of neutrino mixing on the basis of symmetry considerations. In this approach one exploits the fact that, up to perturbative corrections, the PMNS matrix has an approximate form, U_ν , which can be dictated by symmetries. The matrix U_ν is assumed to originate from the diagonalisation of the neutrino Majorana mass term. The angles in U_ν have specific symmetry values which differ, in general, from the experimentally determined values of the PMNS angles θ_{12} , θ_{13} and θ_{23} , and thus need to be corrected. The requisite perturbative corrections, which modify the values of the angles in U_ν to coincide with the measured values of θ_{12} , θ_{13} and θ_{23} , are provided by the matrix U_e arising from the diagonalisation of the charged lepton mass matrix, $U = U_e^\dagger U_\nu$. In the sum rules we will analyse in detail in the present article the Dirac phase δ is expressed, in general, in terms of the mixing angles θ_{12} , θ_{13} and θ_{23} of the PMNS matrix U and the angles present in U_ν , whose values are fixed, being dictated by an underlying approximate symmetry of the lepton sector (see, e.g., [17]).

2 The Sum Rules

In the framework of the reference 3 flavour neutrino mixing we will consider, the PMNS neutrino mixing matrix is always given by

$$U = U_e^\dagger U_\nu, \quad (6)$$

where U_e and U_ν are 3×3 unitary matrices originating from the diagonalisation of the charged lepton and the neutrino (Majorana) mass terms. As we have already indicated, we will suppose in what follows that U_ν has a form which is dictated by symmetries. More specifically, we will assume that

$$U_\nu = \Psi_1 \tilde{U}_\nu Q_0 = \Psi_1 R_{23}(\theta_{23}^\nu) R_{12}(\theta_{12}^\nu) Q_0, \quad (7)$$

where $R_{23}(\theta_{23}^\nu)$ and $R_{12}(\theta_{12}^\nu)$ are orthogonal matrices describing rotations in the 2-3 and 1-2 planes, respectively, and Ψ_1 and Q_0 are diagonal phase matrices each containing two phases. Obviously, the phases in the matrix Q_0 give contribution to the Majorana phases in the PMNS matrix. In the present article we will consider the following symmetry forms of the matrix \tilde{U}_ν : i) tri-bimaximal (TBM) [20], ii) bimaximal (BM), or due to a symmetry corresponding to the conservation of the lepton charge $L' = L_e - L_\mu - L_\tau$ (LC) [21, 22], iii) golden ratio type A (GRA) form [23, 24], iv) golden ratio type B (GRB) form [25], and v) hexagonal (HG) form [26]. In all these cases we have $\theta_{23}^\nu = -\pi/4$ and the matrix \tilde{U}_ν is given by

$$\tilde{U}_\nu = \begin{pmatrix} \cos \theta_{12}^\nu & \sin \theta_{12}^\nu & 0 \\ -\frac{\sin \theta_{12}^\nu}{\sqrt{2}} & \frac{\cos \theta_{12}^\nu}{\sqrt{2}} & -\frac{1}{\sqrt{2}} \\ -\frac{\sin \theta_{12}^\nu}{\sqrt{2}} & \frac{\cos \theta_{12}^\nu}{\sqrt{2}} & \frac{1}{\sqrt{2}} \end{pmatrix}. \quad (8)$$

The TBM, BM (LC), GRA, GRB and HG forms of \tilde{U}_ν correspond to different fixed values of θ_{12}^ν and thus of $\sin^2 \theta_{12}^\nu$, namely, to i) $\sin^2 \theta_{12}^\nu = 1/3$, ii) $\sin^2 \theta_{12}^\nu = 1/2$, iii) $\sin^2 \theta_{12}^\nu =$

$(2+r)^{-1} \cong 0.276$, r being the golden ratio, $r = (1 + \sqrt{5})/2$, iv) $\sin^2 \theta_{12}^\nu = (3-r)/4 \cong 0.345$, and v) $\sin^2 \theta_{12}^\nu = 1/4$. Thus, the matrix U_e in eq. (6) should provide corrections which not only generate nonzero value of θ_{13} , but also lead to reactor, atmospheric and solar neutrino mixing angles θ_{13} , θ_{23} and θ_{12} which have values compatible with the current data, including a possible sizable deviation of θ_{23} from $\pi/4$. As was shown in [13], the minimal form of U_e , in terms of angles and phases it contains, that can provide the requisite corrections to U_ν includes a product of two orthogonal matrices describing rotations in the 2-3 and 1-2 planes, $R_{23}(\theta_{23}^e)$ and $R_{12}(\theta_{12}^e)$, θ_{23}^e and θ_{12}^e being two (real) angles. In what follows we will adopt this minimal form of U_e . It proves convenient to cast it in the form [13]:

$$U_e = \Psi_2^\dagger \tilde{U}_e = \Psi_2^\dagger R_{23}^{-1}(\theta_{23}^e) R_{12}^{-1}(\theta_{12}^e), \quad (9)$$

where Ψ_2 is a diagonal phase matrix including two phases and

$$R_{12}(\theta_{12}^e) = \begin{pmatrix} \cos \theta_{12}^e & \sin \theta_{12}^e & 0 \\ -\sin \theta_{12}^e & \cos \theta_{12}^e & 0 \\ 0 & 0 & 1 \end{pmatrix}, \quad R_{23}(\theta_{23}^e) = \begin{pmatrix} 1 & 0 & 0 \\ 0 & \cos \theta_{23}^e & \sin \theta_{23}^e \\ 0 & -\sin \theta_{23}^e & \cos \theta_{23}^e \end{pmatrix}. \quad (10)$$

Thus, the PMNS matrix in the approach we are following is given by

$$U = U_e^\dagger U_\nu = R_{12}(\theta_{12}^e) R_{23}(\theta_{23}^e) \Psi R_{23}(\theta_{23}^\nu) R_{12}(\theta_{12}^\nu) Q_0, \quad \Psi = \Psi_2 \Psi_1, \quad \theta_{23}^\nu = -\frac{\pi}{4}. \quad (11)$$

The matrices Ψ and Q_0 are diagonal phase matrices each containing, in general, two physical CPV phases³ [27]:

$$\Psi = \text{diag} \left(1, e^{-i\psi}, e^{-i\omega} \right), \quad Q_0 = \text{diag} \left(1, e^{i\frac{\xi_{21}}{2}}, e^{i\frac{\xi_{31}}{2}} \right). \quad (12)$$

The fact that \tilde{U}_e does not include also the orthogonal matrix describing the rotation in the 1-3 plane, $R_{13}(\theta_{13}^e)$, i.e., that θ_{13}^e is negligible, $\theta_{13}^e \cong 0$, follows from the requirement that U_e has a ‘‘minimal’’ form in terms of angles and phases it contains, needed to provide the requisite corrections to U_ν , as was explained earlier. However, $\theta_{13}^e \cong 0$ is a feature of many theories and models of charged lepton mass generation (see, e.g., [16, 23, 28–35]) and was used in a large number of articles dedicated to the problem of understanding the origins of the observed pattern of neutrino mixing (see, e.g., [15, 19, 27, 33, 36–38]). In large class of GUT inspired models of flavour, for instance, the matrix U_e is directly related to the quark mixing matrix (see, e.g., [29, 31, 32, 39, 40]). As a consequence, in this class of models, in particular, θ_{13}^e is negligibly small.

As was shown in [13], the product of matrices $R_{23}(\theta_{23}^e) \Psi R_{23}(\theta_{23}^\nu = -\pi/4)$ in the expression (11) for U_{PMNS} can be rearranged as follows:

$$R_{23}(\theta_{23}^e) \Psi R_{23}(\theta_{23}^\nu = -\pi/4) = P_1 \Phi R_{23}(\hat{\theta}_{23}) Q_1. \quad (13)$$

Here the angle $\hat{\theta}_{23}$ is determined by

$$\sin^2 \hat{\theta}_{23} = \frac{1}{2} (1 - 2 \sin \theta_{23}^e \cos \theta_{23}^e \cos(\omega - \psi)), \quad (14)$$

³The diagonal phase matrix Ψ , as we see, can originate from the charged lepton or the neutrino sector, or else can receive contributions from both sectors [27].

and

$$P_1 = \text{diag}(1, 1, e^{-i\alpha}), \quad \Phi = \text{diag}(1, e^{i\phi}, 1), \quad Q_1 = \text{diag}(1, 1, e^{i\beta}), \quad (15)$$

where

$$\alpha = \gamma + \psi + \omega, \quad \beta = \gamma - \phi, \quad (16)$$

and

$$\gamma = \arg\left(-e^{-i\psi} \cos \theta_{23}^e + e^{-i\omega} \sin \theta_{23}^e\right), \quad \phi = \arg\left(e^{-i\psi} \cos \theta_{23}^e + e^{-i\omega} \sin \theta_{23}^e\right). \quad (17)$$

The phase α in the matrix P_1 is unphysical (it can be absorbed in the τ lepton field). The phase β contributes to the matrix of physical Majorana phases, which now is equal to $\hat{Q} = Q_1 Q_0$. The PMNS matrix takes the form:

$$U_{\text{PMNS}} = R_{12}(\theta_{12}^e) \Phi(\phi) R_{23}(\hat{\theta}_{23}) R_{12}(\theta_{12}^\nu) \hat{Q}, \quad (18)$$

where θ_{12}^ν has a fixed value which depends on the symmetry form of \tilde{U}_ν used. Using eq. (18) we get for the angles θ_{12} , θ_{23} and θ_{13} of the standard parametrisation of the PMNS matrix U [13]:

$$\sin \theta_{13} = |U_{e3}| = \sin \theta_{12}^e \sin \hat{\theta}_{23}, \quad (19)$$

$$\sin^2 \theta_{23} = \frac{|U_{\mu 3}|^2}{1 - |U_{e3}|^2} = \sin^2 \hat{\theta}_{23} \frac{\cos^2 \theta_{12}^e}{1 - \sin^2 \theta_{12}^e \sin^2 \hat{\theta}_{23}} = \frac{\sin^2 \hat{\theta}_{23} - \sin^2 \theta_{13}}{1 - \sin^2 \theta_{13}}, \quad (20)$$

$$\begin{aligned} \sin^2 \theta_{12} = \frac{|U_{e2}|^2}{1 - |U_{e3}|^2} = (1 - \cos^2 \theta_{23} \cos^2 \theta_{13})^{-1} & \left[\sin^2 \theta_{12}^\nu \sin^2 \theta_{23} \right. \\ & \left. + \cos^2 \theta_{12}^\nu \cos^2 \theta_{23} \sin^2 \theta_{13} + \frac{1}{2} \sin 2\theta_{12}^\nu \sin 2\theta_{23} \sin \theta_{13} \cos \phi \right], \quad (21) \end{aligned}$$

where eq. (19) was used in order to obtain the expression for $\sin^2 \theta_{23}$ in terms of $\hat{\theta}_{23}$ and θ_{13} , and eqs. (19) and (20) were used to get the last expression for $\sin^2 \theta_{12}$. The expressions in eqs. (19) - (21) are exact.

It follows from eqs. (1), (2) and (18) that the four observables θ_{12} , θ_{23} , θ_{13} and δ are functions of three parameters θ_{12}^e , $\hat{\theta}_{23}$ and ϕ . As a consequence, the Dirac phase δ can be expressed as a function of the three PMNS angles θ_{12} , θ_{23} and θ_{13} , leading to a new ‘‘sum rule’’ relating δ and θ_{12} , θ_{23} and θ_{13} [13]. For an arbitrary fixed value of the angle θ_{12}^ν the sum rule for $\cos \delta$ reads [14]:

$$\cos \delta = \frac{\tan \theta_{23}}{\sin 2\theta_{12} \sin \theta_{13}} \left[\cos 2\theta_{12}^\nu + (\sin^2 \theta_{12} - \cos^2 \theta_{12}^\nu) (1 - \cot^2 \theta_{23} \sin^2 \theta_{13}) \right]. \quad (22)$$

A similar sum rule can be derived for the phases ϕ [13,14]. It proves convenient for our further discussion to cast the sum rules for $\cos \delta$ and $\cos \phi$ in the form:

$$\sin^2 \theta_{12} = \cos^2 \theta_{12}^\nu + \frac{\sin 2\theta_{12} \sin \theta_{13} \cos \delta - \tan \theta_{23} \cos 2\theta_{12}^\nu}{\tan \theta_{23} (1 - \cot^2 \theta_{23} \sin^2 \theta_{13})}, \quad (23)$$

$$\sin^2 \theta_{12} = \cos^2 \theta_{12}^\nu + \sin^2 \theta_{23} \frac{\sin 2\theta_{12}^\nu \sin \theta_{13} \cos \phi - \cos 2\theta_{12}^\nu}{(1 - \cos^2 \theta_{23} \cos^2 \theta_{13})}. \quad (24)$$

The phases δ and ϕ are related by [14]

$$\sin \delta = - \frac{\sin 2\theta_{12}^\nu}{\sin 2\theta_{12}} \sin \phi, \quad (25)$$

$$\begin{aligned} \cos \delta = & \frac{\sin 2\theta_{12}^\nu}{\sin 2\theta_{12}} \cos \phi \left(-1 + \frac{2 \sin^2 \theta_{23}}{\sin^2 \theta_{23} \cos^2 \theta_{13} + \sin^2 \theta_{13}} \right) \\ & + \frac{\cos 2\theta_{12}^\nu}{\sin 2\theta_{12}} \frac{\sin 2\theta_{23} \sin \theta_{13}}{\sin^2 \theta_{23} \cos^2 \theta_{13} + \sin^2 \theta_{13}}. \end{aligned} \quad (26)$$

The sum rules (22) - (24) and the relations (25) and (26) are exact.

A parametrisation of the PMNS matrix, similar to that given in eq. (11), has been effectively employed in ref. [15]: the hierarchy of values of the angles in the matrices U_e and U_ν assumed in [15] leads the authors to consider the angles θ_{13}^e and θ_{13}^ν of the 1-3 rotations in U_e and U_ν as negligibly small. As a consequence, the PMNS matrix is effectively parametrised in [15] with four angles $\theta_{12}^e, \theta_{23}^e, \theta_{12}^\nu, \theta_{23}^\nu$ and ⁴ four phases $\delta_{12}^e, \delta_{23}^e, \delta_{12}^\nu, \delta_{23}^\nu$. As is shown in Appendix A (see also ref. [14]), these phases are related to the phases ψ, ω, ξ_{21} and ξ_{31} present in the parametrisation in eq. (11) as follows:

$$\psi = \delta_{12}^e - \delta_{12}^\nu + \pi, \quad \omega = \delta_{23}^e + \delta_{12}^e - \delta_{23}^\nu - \delta_{12}^\nu, \quad (27)$$

$$\xi_{21} = -2\delta_{12}^\nu, \quad \xi_{31} = -2(\delta_{12}^\nu + \delta_{23}^\nu). \quad (28)$$

Treating $\sin \theta_{12}^e$ and $\sin \theta_{23}^e$ as small parameters, $|\sin \theta_{12}^e| \ll 1, |\sin \theta_{23}^e| \ll 1$, neglecting terms of order of, or smaller than, $O((\theta_{12}^e)^2), O((\theta_{23}^e)^2)$ and $O(\theta_{12}^e \theta_{23}^e)$, and taking into account that in this approximation we have $\sin \theta_{12}^e = \sqrt{2} \sin \theta_{13}$, the following ‘‘leading order’’ sum rule was obtained in [15]:

$$\theta_{12} \approx \theta_{12}^\nu + \theta_{13} \cos \delta. \quad (29)$$

This sum rule can be derived from the sum rule

$$\sin \theta_{12} \approx \sin \theta_{12}^\nu + \frac{\sin 2\theta_{12}^\nu}{2 \sin \theta_{12}^\nu} \sin \theta_{13} \cos \delta, \quad (30)$$

by treating $\sin 2\theta_{12}^\nu \sin \theta_{13} \cos \delta \cong \sin 2\theta_{12}^\nu \theta_{13} \cos \delta$ as a small parameter and using the Taylor expansion $\sin^{-1}(a + bx) \approx \sin^{-1}(a) + bx/\sqrt{1 - a^2}$, valid for $|bx| \ll 1$.

From eqs. (23) and (24), employing the approximations used in ref. [15], we get:

$$\sin^2 \theta_{12} \cong \sin^2 \theta_{12}^\nu + \sin 2\theta_{12} \sin \theta_{13} \cos \delta, \quad (31)$$

$$\sin^2 \theta_{12} \cong \sin^2 \theta_{12}^\nu + \sin 2\theta_{12}^\nu \sin \theta_{13} \cos \phi. \quad (32)$$

The first equation leads (in the leading order approximation used to derive it and using $\sin 2\theta_{12} \cong \sin 2\theta_{12}^\nu$) to eq. (29), while from the second equation we find

$$\sin \theta_{12} \cong \sin \theta_{12}^\nu + \frac{\sin 2\theta_{12}^\nu}{2 \sin \theta_{12}^\nu} \sin \theta_{13} \cos \phi, \quad (33)$$

and correspondingly,

$$\theta_{12} \approx \theta_{12}^\nu + \theta_{13} \cos \phi. \quad (34)$$

⁴In contrast to $\theta_{23}^\nu = \pi/4$ employed in [15], we use $\theta_{23}^\nu = -\pi/4$. The effect of the difference in the signs of $\sin \theta_{12}^e$ and $\sin \theta_{23}^e$ utilised by us and in [15] is discussed in Appendix A.

This implies that in the leading order approximation adopted in ref. [15] we have [14] $\cos \delta = \cos \phi$. Note, however, that the sum rules for $\cos \delta$ and $\cos \phi$ given in eqs. (31) and (32), differ somewhat by the factors multiplying the terms $\propto \sin \theta_{13}$.

As was shown in [14], the leading order sum rule (29) leads in the cases of TBM, GRA, GRB and HG forms of \tilde{U}_ν to largely imprecise predictions for the value of $\cos \delta$: for the best fit values of $\sin^2 \theta_{12} = 0.308$, $\sin^2 \theta_{13} = 0.0234$ and $\sin^2 \theta_{23} = 0.425$ used in [14], they differ approximately by factors (1.4 - 1.9) from the values found from the exact sum rule. The same result holds for $\cos \phi$. Moreover, the predicted values of $\cos \delta$ and $\cos \phi$ differ approximately by factors of (1.5 - 2.0), in contrast to the prediction $\cos \delta \cong \cos \phi$ following from the leading order sum rules. The large differences between the results for $\cos \delta$ and $\cos \phi$, obtained using the leading order and the exact sum rules, are a consequence [14] of the quantitative importance of the next-to-leading order terms which are neglected in the leading order sum rules (29) - (34). The next-to-leading order terms are significant for the TBM, GRA, GRB and HG forms of \tilde{U}_ν , because in all these cases the ‘‘dominant’’ terms $|\theta_{12} - \theta_{12}^\nu| \sim \sin^2 \theta_{13}$, or equivalently ⁵ $|\sin^2 \theta_{12} - \sin^2 \theta_{12}^\nu| \sim \sin^2 \theta_{13}$. It was shown also in [14] that in the case of BM (LC) form of \tilde{U}_ν we have $|\theta_{12} - \theta_{12}^\nu| \sim \sin \theta_{13}$ and the leading order sum rules provide rather precise predictions for $\cos \delta$ and $\cos \phi$.

The results quoted above were obtained in [14] for the best fit values of the neutrino mixing parameters $\sin^2 \theta_{12}$, $\sin^2 \theta_{23}$ and $\sin^2 \theta_{13}$. In the present article we investigate in detail the predictions for $\cos \delta$ and $\cos \phi$ in the cases of TBM, BM (LC), GRA, GRB and HG forms of \tilde{U}_ν using the exact sum rules given in eqs. (23) (or (22)) and (24) and the leading order sum rules in eqs. (31) and (32), taking into account also the uncertainties in the measured values of $\sin^2 \theta_{12}$, $\sin^2 \theta_{23}$ and $\sin^2 \theta_{13}$. This allows us to better assess the accuracy of the predictions for $\cos \delta$ and $\cos \phi$ based on the leading order sum rules and its dependence on the values of neutrino mixing angles. We investigate also how the predictions for $\cos \delta$ and $\cos \phi$, obtained using the exact and the leading order sum rules, vary when the PMNS neutrino mixing parameters $\sin^2 \theta_{12}$, $\sin^2 \theta_{23}$ and $\sin^2 \theta_{13}$ are varied in their respective experimentally allowed 3σ ranges.

In what follows we will present numerical results using the values of $\sin^2 \theta_{12}$, $\sin^2 \theta_{23}$ and $\sin^2 \theta_{13}$ quoted in eqs. (3) - (5) and corresponding to the NO spectrum of neutrino masses. The results we obtain in the case of IO spectrum differ insignificantly from those found for the NO spectrum.

3 The Case of Negligible θ_{23}^e

The case of negligible $\theta_{23}^e \cong 0$ was investigated by many authors (see, e.g., [15, 16, 19, 29, 30, 36, 37, 41]). It corresponds to a large number of theories and models of charged lepton and neutrino mass generation (see, e.g., [16, 29–33]). For $\theta_{23}^e \cong 0$, the sum rules of interest given in eqs. (23) (or (22)), (24) and in eqs. (31), (32) were analysed in detail in ref. [14].

In the limit of negligibly small θ_{23}^e we find from eqs. (14), (16) and (17):

$$\sin^2 \hat{\theta}_{23} = \frac{1}{2}, \quad \gamma = -\psi + \pi, \quad \phi = -\psi = \delta_{12}^\nu - \delta_{12}^e - \pi, \quad \beta = \gamma - \phi = \pi. \quad (35)$$

The phase ω is unphysical.

⁵Note that [14] since $\cos \delta$ and $\cos \phi$ in eqs. (29) - (34) are multiplied by $\sin \theta_{13}$, the ‘‘dominant’’ terms $|\theta_{12} - \theta_{12}^\nu|$ and the next-to-leading order terms $\sim \sin^2 \theta_{13}$ give contributions to $\cos \delta$ and $\cos \phi$, which are both of the same order and are $\sim \sin \theta_{13}$.

In the limiting case of negligible θ_{23}^e the exact sum rules for $\cos \delta$ and $\cos \phi$ take the following form [14]:

$$\cos \delta = \frac{(1 - 2 \sin^2 \theta_{13})^{\frac{1}{2}}}{\sin 2\theta_{12} \sin \theta_{13}} \left[\cos 2\theta_{12}^\nu + (\sin^2 \theta_{12} - \cos^2 \theta_{12}^\nu) \frac{1 - 3 \sin^2 \theta_{13}}{1 - 2 \sin^2 \theta_{13}} \right], \quad (36)$$

$$\cos \phi = \frac{1 - \sin^2 \theta_{13}}{\sin 2\theta_{12}^\nu \sin \theta_{13} (1 - 2 \sin^2 \theta_{13})^{\frac{1}{2}}} \left[\sin^2 \theta_{12} - \sin^2 \theta_{12}^\nu - \cos 2\theta_{12}^\nu \frac{\sin^2 \theta_{13}}{1 - \sin^2 \theta_{13}} \right]. \quad (37)$$

From the above equations, to leading order in $\sin \theta_{13}$ we get:

$$\cos \delta = \frac{1}{\sin 2\theta_{12} \sin \theta_{13}} (\sin^2 \theta_{12} - \sin^2 \theta_{12}^\nu) + O(\sin \theta_{13}), \quad (38)$$

$$\cos \phi = \frac{1}{\sin 2\theta_{12}^\nu \sin \theta_{13}} (\sin^2 \theta_{12} - \sin^2 \theta_{12}^\nu) + O(\sin \theta_{13}), \quad (39)$$

or equivalently,

$$\sin^2 \theta_{12} = \sin^2 \theta_{12}^\nu + \sin 2\theta_{12} \sin \theta_{13} \cos \delta + O(\sin^2 \theta_{13}), \quad (40)$$

$$\sin^2 \theta_{12} = \sin^2 \theta_{12}^\nu + \sin 2\theta_{12}^\nu \sin \theta_{13} \cos \phi + O(\sin^2 \theta_{13}). \quad (41)$$

The last two equations coincide with eqs. (31) and (32) which were derived from the exact sum rules keeping the leading order corrections in both $\sin \theta_{13}$ and $\sin \theta_{23}^e$. This implies, in particular, that the correction due to $|\sin \theta_{23}^e| \ll 1$ appears in the sum rules of interest only in the next-to-leading order terms. Casting the results obtained in a form we are going to use in our numerical analysis we obtain:

$$\sin \theta_{12} = \sin \theta_{12}^\nu + \frac{\sin 2\theta_{12}}{2 \sin \theta_{12}^\nu} \sin \theta_{13} \cos \delta + O(\sin^2 \theta_{13}) \quad (42)$$

$$= \sin \theta_{12}^\nu + \frac{\sin 2\theta_{12}^\nu}{2 \sin \theta_{12}^\nu} \sin \theta_{13} \cos \delta + O(\sin^2 \theta_{13}), \quad (43)$$

$$\sin \theta_{12} = \sin \theta_{12}^\nu + \frac{\sin 2\theta_{12}^\nu}{2 \sin \theta_{12}^\nu} \sin \theta_{13} \cos \phi + O(\sin^2 \theta_{13}). \quad (44)$$

We have replaced $\sin 2\theta_{12}$ with $\sin 2\theta_{12}^\nu$ in eq. (43), so that it corresponds to eqs. (29) and (30). In the cases of the TBM, GRA, GRB and HG symmetry forms of \tilde{U}_ν we are considering and for the best fit value of $\sin^2 \theta_{12} = 0.308$ we indeed have $|\sin \theta_{12} - \sin \theta_{12}^\nu| \sim \sin^2 \theta_{13}$. Thus, if one applies consistently the approximations employed in [15], which lead to eqs. (29) - (34) (or to eqs. (38) and (39)), one should neglect also the difference between θ_{12} and θ_{12}^ν . This leads to $\cos \delta = \cos \phi = 0$.

In Fig. 1 we show predictions for $\cos \delta$ and $\cos \phi$ in the cases of TBM, GRA, GRB and HG forms of the matrix \tilde{U}_ν , as functions of $\sin \theta_{13}$ which is varied in the 3σ interval given in eq. (5) and corresponding to NO neutrino mass spectrum. The predictions are obtained for the best fit value of $\sin^2 \theta_{12} = 0.308$ using the exact sum rules (36) and (37) for $\cos \delta$ (solid lines) and $\cos \phi$ (dashed lines) and the leading order sum rules (43) and (44) (dash-dotted lines). As we see in Fig. 1, the predictions for $\cos \delta$ vary in magnitude and sign when one varies the symmetry form of \tilde{U}_ν . More specifically, from the exact sum rule in eq. (36), using the best

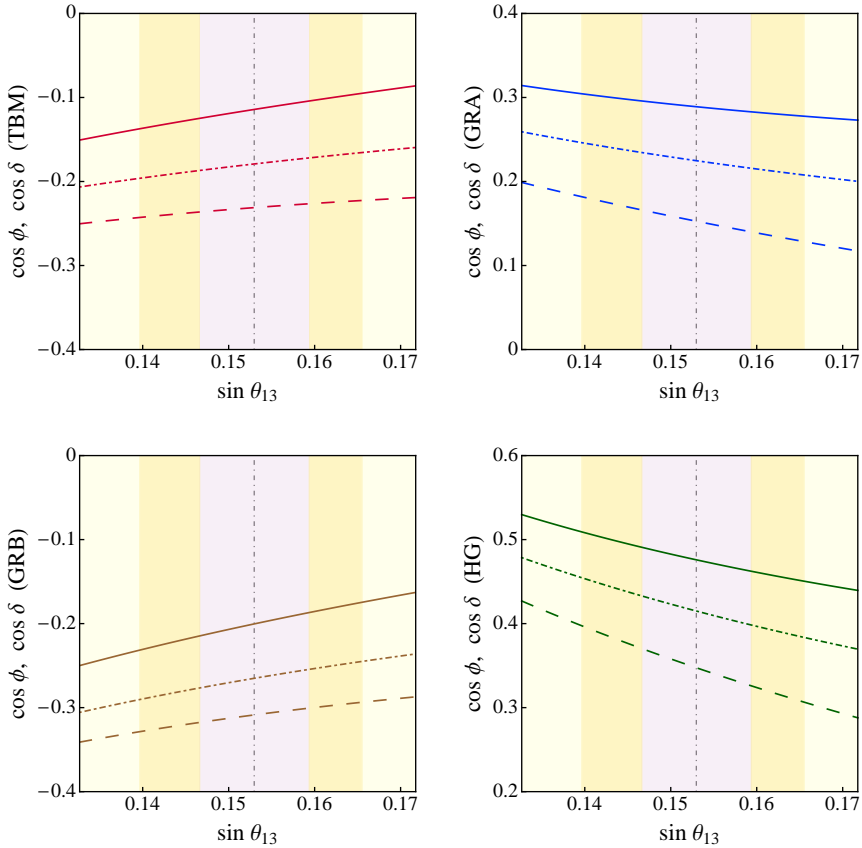


Figure 1: Predictions for $\cos \delta$ and $\cos \phi$ in the cases of TBM (upper left panel), GRA (upper right panel), GRB (lower left panel) and HG (lower right panel) forms of the matrix \tilde{U}_ν , as functions of $\sin \theta_{13}$ and for the best fit value of $\sin^2 \theta_{12} = 0.308$. The solid lines (dashed lines) correspond to $\cos \delta$ ($\cos \phi$) determined from the exact sum rule given in eq. (36) (eq. (37)). The dash-dotted line in each of the 4 panels represents $(\cos \delta)_{\text{LO}} = (\cos \phi)_{\text{LO}}$ obtained from the leading order sum rule in eq. (43). The vertical dash-dotted line corresponds to the best fit value of $\sin^2 \theta_{13} = 0.0234$; the three colored vertical bands indicate the 1σ , 2σ and 3σ experimentally allowed ranges of $\sin \theta_{13}$ (see text for further details).

fit value of $\sin^2 \theta_{13} = 0.0234$ we get for $\cos \delta$ in the cases of the TBM, BM (LC), GRA, GRB and HG forms of \tilde{U}_ν , respectively: $\cos \delta = (-0.114)$; (-1.29) ; 0.289 ; (-0.200) ; 0.476 .

The unphysical value of $\cos \delta$ in the case of the BM (LC) form of \tilde{U}_ν is a reflection of the fact that the scheme under discussion with BM (LC) form of the matrix \tilde{U}_ν does not provide a good description of the current data on θ_{12} , θ_{23} and θ_{13} [13]. One gets a physical result for $\cos \delta$, $\cos \delta = -0.973$, for, e.g., values of $\sin^2 \theta_{12} = 0.32$, and $\sin \theta_{13} = 0.16$, lying in the 2σ experimentally allowed intervals of these neutrino mixing parameters. We have checked that for the best fit value of $\sin^2 \theta_{13}$, physical values of $(\cos \delta)_{\text{E}}$, $(\cos \delta)_{\text{LO}}$ and $(\cos \phi)_{\text{E}}$ in the BM (LC) case can be obtained for relatively large values of $\sin^2 \theta_{12}$. For, e.g., $\sin^2 \theta_{12} = 0.359$ and $\sin^2 \theta_{13} = 0.0234$ we find $(\cos \delta)_{\text{E}} = -0.915$, $(\cos \delta)_{\text{LO}} = -0.998$ and $(\cos \phi)_{\text{E}} = -0.922$. In this case the differences between the exact and leading order sum rule results for $\cos \delta$ and $\cos \phi$ are relatively small.

$\sin^2 \theta_{12} = 0.308$	TBM	GRA	GRB	HG
$(\cos \delta)_E$	-0.114	0.289	-0.200	0.476
$(\cos \delta)_{LO}$	-0.179	0.225	-0.265	0.415
$(\cos \delta)_E/(\cos \delta)_{LO}$	0.638	1.29	0.756	1.15
$(\cos \phi)_E$	-0.231	0.153	-0.309	0.347
$(\cos \delta)_E/(\cos \phi)_E$	0.494	1.89	0.649	1.37
$(\cos \phi)_E/(\cos \phi)_{LO}$	1.29	0.680	1.16	0.837

Table 1: The predicted values of $\cos \delta$ and $\cos \phi$, obtained from the exact sum rules in eqs. (36) and (37), $(\cos \delta)_E$ and $(\cos \phi)_E$, and from the leading order sum rule in eq. (43), $(\cos \delta)_{LO} = (\cos \phi)_{LO}$, using the best fit values of $\sin^2 \theta_{13} = 0.0234$ and $\sin^2 \theta_{12} = 0.308$, for the TBM, GRA, GRB and HG forms of the matrix \tilde{U}_ν . The values of the ratios $(\cos \delta)_E/(\cos \delta)_{LO}$, $(\cos \delta)_E/(\cos \phi)_E$ and $(\cos \phi)_E/(\cos \phi)_{LO}$ are also shown.

The above results imply that it would be possible to distinguish between the different symmetry forms of \tilde{U}_ν considered by measuring $\cos \delta$ [14], provided $\sin^2 \theta_{12}$ is known with sufficiently high precision. Even determining the sign of $\cos \delta$ will be sufficient to eliminate some of the possible symmetry forms of \tilde{U}_ν .

The leading order sum rules (43) and (44) lead to values of $\cos \delta$ and $\cos \phi$, $(\cos \delta)_{LO}$ and $(\cos \phi)_{LO}$, which coincide: $(\cos \delta)_{LO} = (\cos \phi)_{LO}$. These values differ, however, from the values obtained employing the exact sum rules: $(\cos \delta)_E \neq (\cos \delta)_{LO}$, $(\cos \phi)_E \neq (\cos \phi)_{LO}$. The exact sum rule values of $\cos \delta$ and $\cos \phi$ also differ: $(\cos \delta)_E \neq (\cos \phi)_E$. We are interested both in the predictions for the values of $(\cos \delta)_E$, $(\cos \delta)_{LO}$, $(\cos \phi)_E$ and $(\cos \phi)_{LO}$, and in the differences between the exact and the leading order sum rule predictions. In Table 1 we give the values of $(\cos \delta)_E$, $(\cos \phi)_E$, $(\cos \delta)_{LO} = (\cos \phi)_{LO}$, and of the ratios $(\cos \delta)_E/(\cos \phi)_E$, $(\cos \delta)_E/(\cos \delta)_{LO}$ and $(\cos \phi)_E/(\cos \phi)_{LO}$, calculated for the best fit values of $\sin^2 \theta_{13} = 0.0234$ and $\sin^2 \theta_{12} = 0.308$.

As Fig. 1 indicates, the differences $|(\cos \delta)_E - (\cos \delta)_{LO}|$ and $|(\cos \phi)_E - (\cos \phi)_{LO}|$ exhibit weak dependence on the value of $\sin \theta_{13}$ when it is varied in the 3σ interval quoted in eq. (5). The values of $\cos \delta$, obtained using the exact sum rule (36) in the TBM, GRA, GRB and HG cases, differ from those calculated using the approximate sum rule (43) by the factors 0.638, 1.29, 0.756 and 1.15, respectively. The largest difference is found to hold in the TBM case. As was shown in [14], the correction to $(\cos \delta)_{LO}$ - the leading order sum rule result for $\cos \delta$ - is given approximately by $\cos 2\theta'_{12} \sin \theta_{13}$. For given θ'_{12} , the relative magnitude of the correction depends on the magnitude of the ratio $|\sin^2 \theta_{12} - \sin^2 \theta'_{12}|/\sin \theta_{13}$. The largest correction occurs for the symmetry form of \tilde{U}_ν , for which this ratio has the smallest value. For the best fit value of $\sin^2 \theta_{12}$, the smallest value of the ratio of interest corresponds to the TBM form of \tilde{U}_ν and is equal approximately to 0.166.

The behavior of $\cos \delta$ and $\cos \phi$ when $\sin \theta_{13}$ increases is determined by the sign of $(\sin^2 \theta_{12} - \sin^2 \theta'_{12})$: $\cos \delta$ and $\cos \phi$ increase (decrease) when this difference is negative (positive). For the best fit value of $\sin^2 \theta_{12} = 0.308$, this difference is negative in the TBM and GRB cases, while it is positive in the GRA and HG ones. For the four symmetry forms of \tilde{U}_ν , TBM, GRB, GRA and HG, and the best fit values of $\sin^2 \theta_{13} = 0.0234$ and $\sin^2 \theta_{12} = 0.308$, the ratio $(\sin^2 \theta_{12} - \sin^2 \theta'_{12})/\sin \theta_{13}$ reads, respectively: (-0.166) , (-0.245) , 0.207 and 0.379 .

Given the fact that the magnitude of the ratio $(\sin^2 \theta_{12} - \sin^2 \theta'_{12})/\sin \theta_{13}$ determines the factor by which $(\cos \delta)_E$ and $(\cos \delta)_{LO}$ (and $(\cos \phi)_E$ and $(\cos \phi)_{LO}$) differ, we have checked

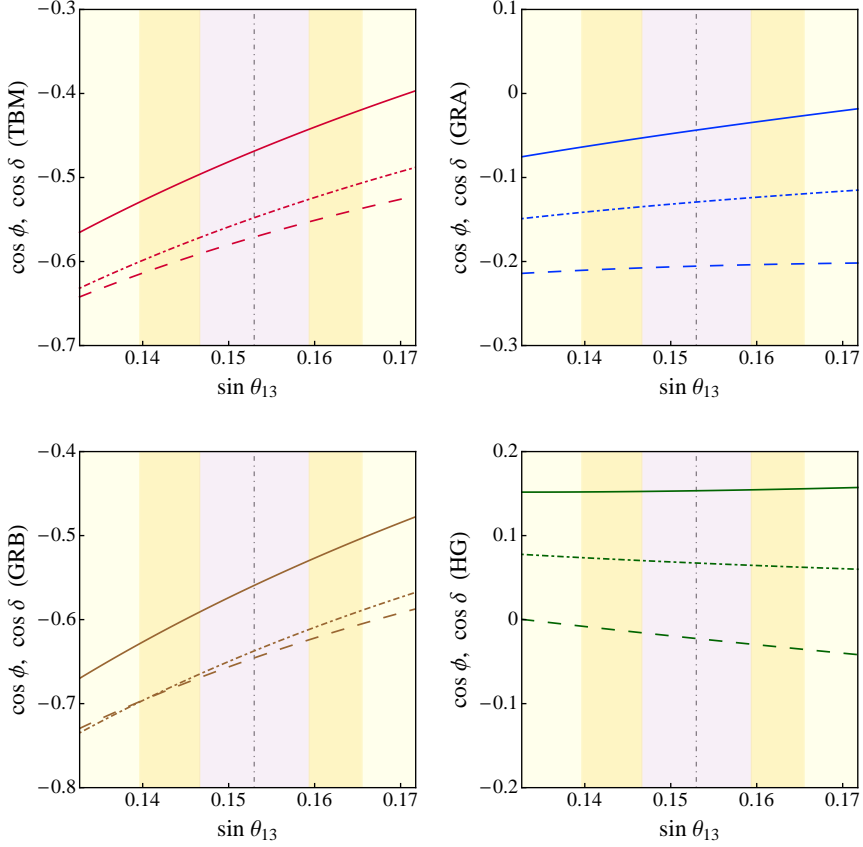


Figure 2: The same as in Fig. 1, but for $\sin^2 \theta_{12} = 0.259$ (see text for further details).

how the results described above change when $\sin^2 \theta_{12}$ is varied in its 3σ allowed region, eq. (3). In Figs. 2 and 3 we show the dependence of the predicted values of $(\cos \delta)_E$, $(\cos \phi)_E$ and $(\cos \delta)_{LO} = (\cos \phi)_{LO}$ on $\sin \theta_{13}$ for the minimal and maximal 3σ allowed values of $\sin^2 \theta_{12}$, $\sin^2 \theta_{12} = 0.259$ and 0.359 . The results shown correspond to the TBM, GRA, GRB, HG forms of \tilde{U}_ν . For $\sin^2 \theta_{12} = 0.259$ ($\sin^2 \theta_{12} = 0.359$) and $\sin^2 \theta_{13} = 0.0234$, the ratio $(\sin^2 \theta_{12} - \sin^2 \theta'_{12}) / \sin \theta_{13}$ in the TBM, GRA, GRB and HG cases takes respectively the values: (-0.486) , (-0.114) , (-0.565) and 0.059 (0.168 , 0.540 , 0.088 and 0.713). As in the preceding case, we give the predicted values of $(\cos \delta)_E$, $(\cos \phi)_E$, $(\cos \delta)_{LO} = (\cos \phi)_{LO}$, and the ratios between them, for $\sin^2 \theta_{12} = 0.259$ ($\sin^2 \theta_{12} = 0.359$) and $\sin^2 \theta_{13} = 0.0234$ in Table 2 (Table 3).

It follows from the results presented in Tables 1 - 3 that the exact sum rule predictions of $\cos \delta$, $(\cos \delta)_E$, for the three values of $\sin^2 \theta_{12} = 0.308$, 0.259 and 0.359 , differ drastically. For the TBM form of \tilde{U}_ν , for instance, we get, respectively, the values: $(\cos \delta)_E = (-0.114)$, (-0.469) and 0.221 . For the GRA and GRB forms of \tilde{U}_ν we have, respectively, $(\cos \delta)_E = 0.289$, (-0.044) , 0.609 , and $(\cos \delta)_E = (-0.200)$, (-0.559) , 0.138 . Similarly, for the HG form we find for the three values of $\sin^2 \theta_{12}$: $(\cos \delta)_E = 0.476$, 0.153 , 0.789 . Thus, in the cases of the symmetry forms of \tilde{U}_ν considered, the exact sum rule predictions for $\cos \delta$ not only change significantly in magnitude when $\sin^2 \theta_{12}$ is varied in its 3σ allowed range, but also the sign of

$\sin^2 \theta_{12} = 0.259$	TBM	GRA	GRB	HG
$(\cos \delta)_E$	-0.469	-0.0436	-0.559	0.153
$(\cos \delta)_{LO}$	-0.548	-0.129	-0.637	0.0673
$(\cos \delta)_E/(\cos \delta)_{LO}$	0.855	0.338	0.878	2.28
$(\cos \phi)_E$	-0.571	-0.206	-0.646	-0.0225
$(\cos \delta)_E/(\cos \phi)_E$	0.821	0.212	0.866	-6.82
$(\cos \phi)_E/(\cos \phi)_{LO}$	1.04	1.59	1.01	-0.334

Table 2: The same as in Table 1, but for $\sin^2 \theta_{12} = 0.259$.

$\cos \delta$ changes (see Fig. 4).

We observe also that for $\sin^2 \theta_{12} = 0.259$, the values of $\cos \delta$, obtained using the exact sum rule eq. (36) in the TBM, GRA, GRB and HG cases differ from those calculated using the leading order sum rule in eq. (43) by the factors 0.855, 0.338, 0.878 and 2.28, respectively; in the case of $\sin^2 \theta_{12} = 0.359$ the same factors read: 1.27, 1.08, 1.50 and 1.05.

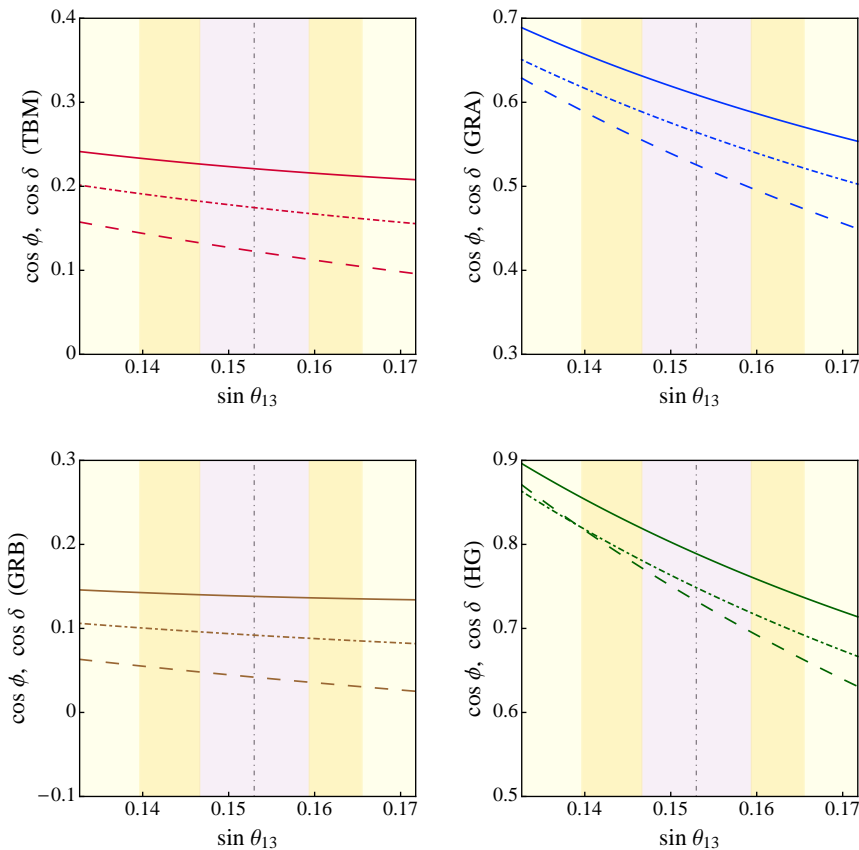


Figure 3: The same as in Fig. 1, but for $\sin^2 \theta_{12} = 0.359$ (see text for further details).

For $\sin^2 \theta_{12} = 0.259$, the largest difference between the exact and leading order sum rule results for $\cos \delta$ occurs for the GRA and HG forms of \tilde{U}_ν , while if $\sin^2 \theta_{12} = 0.359$, the largest

$\sin^2 \theta_{12} = 0.359$	TBM	GRA	GRB	HG
$(\cos \delta)_E$	0.221	0.609	0.138	0.789
$(\cos \delta)_{LO}$	0.175	0.564	0.092	0.749
$(\cos \delta)_E/(\cos \delta)_{LO}$	1.27	1.08	1.50	1.05
$(\cos \phi)_E$	0.123	0.526	0.042	0.733
$(\cos \delta)_E/(\cos \phi)_E$	1.80	1.16	3.29	1.08
$(\cos \phi)_E/(\cos \phi)_{LO}$	0.702	0.931	0.456	0.979

Table 3: The same as in Table 1, but for $\sin^2 \theta_{12} = 0.359$.

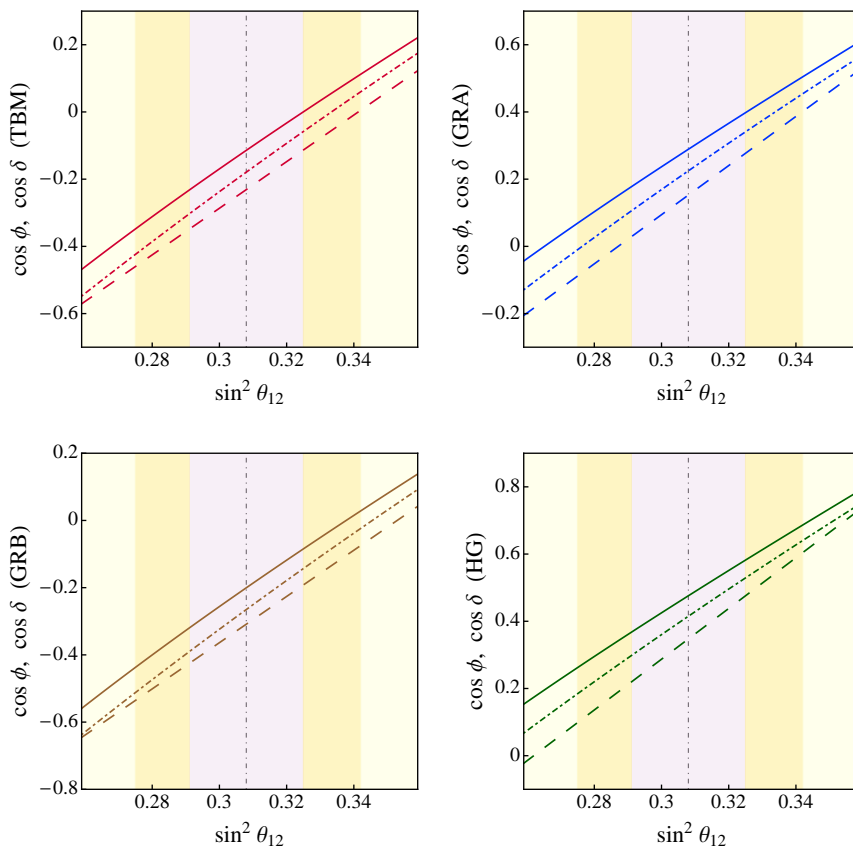


Figure 4: The same as in Fig. 1, but for $\sin^2 \theta_{13} = 0.0234$ and varying $\sin^2 \theta_{12}$ in the 3σ range. The vertical dash-dotted line corresponds to the best fit value of $\sin^2 \theta_{12} = 0.308$ (see text for further details).

difference holds for the TBM and GRB forms.

As Figs. 1 - 3 and Tables 1 - 3 show, similar results are valid for $\cos \phi$ obtained from the exact and the leading order sum rules.

It is worth noting also that the values of $\cos \phi$ and $\cos \delta$, derived from the respective exact sum rules differ significantly for the TBM, GRA, GRB and HG forms of \tilde{U}_ν considered. As pointed out in [14], for the best fit values of $\sin^2 \theta_{13}$ and $\sin^2 \theta_{12}$ they differ by factors (1.5–2.0),

as can be seen also from Table 1. This difference can be much larger for $\sin^2 \theta_{12} = 0.259$ and 0.359 : for these two values of $\sin^2 \theta_{12}$, $\cos \delta$ and $\cos \phi$ differ in the cases of the different symmetry forms of interest approximately by factors $(1.2 - 6.8)$ and $(1.1 - 3.3)$, respectively.

4 The Case of Nonzero θ_{23}^e

For $\theta_{23}^e = 0$ we have in the scheme we are considering: $\theta_{23} \cong \pi/4 - 0.5 \sin^2 \theta_{13}$. A nonzero value of θ_{23}^e allows for a significant deviation of θ_{23} from $\pi/4$. Such deviation is not excluded by the current data on $\sin^2 \theta_{23}$, eq. (4): at 3σ , values of $\sin^2 \theta_{23}$ in the interval $(0.37 - 0.64)$ are allowed, the best fit value being $\sin^2 \theta_{23} = 0.437$ (0.455). The exact sum rules for $\cos \delta$ and $\cos \phi$, eqs. (22), (23) and (24), depend on $\tan \theta_{23}$ and $\sin^2 \theta_{23}$, respectively, while the leading order sum rules, eqs. (29) and (34), do not exhibit any dependence on θ_{23} . In this Section we are going to investigate how the dependence on θ_{23} affects the predictions for $\cos \delta$ and $\cos \phi$, based on the exact sum rules.

We note first that from the exact sum rules in eqs. (23) and (24) we get to leading order in $\sin \theta_{13}$:

$$\sin^2 \theta_{12} = \sin^2 \theta_{12}^\nu + \frac{\sin 2\theta_{12}^\nu}{\tan \theta_{23}} \sin \theta_{13} \cos \delta + O(\sin^2 \theta_{13}), \quad (45)$$

$$\sin^2 \theta_{12} = \sin^2 \theta_{12}^\nu + \frac{\sin 2\theta_{12}^\nu}{\tan \theta_{23}} \sin \theta_{13} \cos \phi + O(\sin^2 \theta_{13}). \quad (46)$$

It follows from eqs. (14) and (20) that in the case of $|\sin \theta_{23}^e| \ll 1$ considered in ref. [15], we have [14] $\tan^{-1} \theta_{23} \cong 2 \cos^2 \theta_{23} = 1 + O(\sin \theta_{23}^e)$. Applying the approximation employed in ref. [15], in which terms of the order of, or smaller than, $\sin^2 \theta_{13}$, $\sin^2 \theta_{23}^e$ and $\sin \theta_{13} \sin \theta_{23}^e$, in the sum rules of interest are neglected, we have to set $\tan^{-1} \theta_{23} = 1$ in eqs. (45) and (46). This leads to eqs. (31) and (32) and, correspondingly, to eqs. (29) and (34).

In Fig. 5 we show the predictions for $\cos \delta$ and $\cos \phi$ in the cases of the TBM, GRA, GRB and HG forms of the matrix \tilde{U}_ν , derived from the exact sum rules in eqs. (23) and (24), $(\cos \delta)_E$ (solid line) and $(\cos \phi)_E$ (dashed line), and from the leading order sum rule in eq. (30) (eq. (33)), $(\cos \delta)_{LO} = (\cos \phi)_{LO}$ (dash-dotted line). The results presented in Fig. 5 are obtained for the best fit values of $\sin^2 \theta_{12} = 0.308$ and $\sin^2 \theta_{23} = 0.437$. The parameter $\sin^2 \theta_{13}$ is varied in its 3σ allowed range, eq. (5). In Table 4 we give the values of $(\cos \delta)_E$, $(\cos \delta)_{LO}$, $(\cos \phi)_E$ and of their ratios, corresponding to the best fit values of $\sin^2 \theta_{12}$, $\sin^2 \theta_{23}$ and $\sin^2 \theta_{13}$. We see from Table 4 that for the TBM, GRA, GRB and HG forms of \tilde{U}_ν , $\cos \delta$ determined from the exact sum rule takes respectively the values (-0.091) , 0.275 , (-0.169) and 0.445 . The values of $\cos \delta$, found using the exact sum rule, eq. (23), differ in the TBM, GRA, GRB and HG cases from those calculated using the leading order sum rule, eq. (30), by the factors 0.506 , 1.22 , 0.636 and 1.07 , respectively. Thus, the largest difference between the predictions of the exact and the leading order sum rules occurs for the TBM form of \tilde{U}_ν .

Since the predictions of the sum rules depend on the value of θ_{12} , we show in Fig. 6 and Fig. 7 also results for the values of $\sin^2 \theta_{12}$, corresponding to the lower and the upper bounds of the 3σ allowed range of $\sin^2 \theta_{12}$, $\sin^2 \theta_{12} = 0.259$ and 0.359 , keeping $\sin^2 \theta_{23}$ fixed to its best fit value. The predictions for $(\cos \delta)_E$, $(\cos \phi)_E$, $(\cos \delta)_{LO} = (\cos \phi)_{LO}$ and their ratios, obtained for the best fit values of $\sin^2 \theta_{13} = 0.0234$ and $\sin^2 \theta_{23} = 0.437$, and for $\sin^2 \theta_{12} = 0.259$ ($\sin^2 \theta_{12} = 0.359$) are given in Table 5 (Table 6). For $\sin^2 \theta_{12} = 0.259$, the exact sum rule predictions of $\cos \delta$ for the TBM, GRA, GRB and HG forms of \tilde{U}_ν read (see Table 5): $(\cos \delta)_E = (-0.408)$, (-0.022) , (-0.490) and 0.156 . As in the case of negligible θ_{23}^e

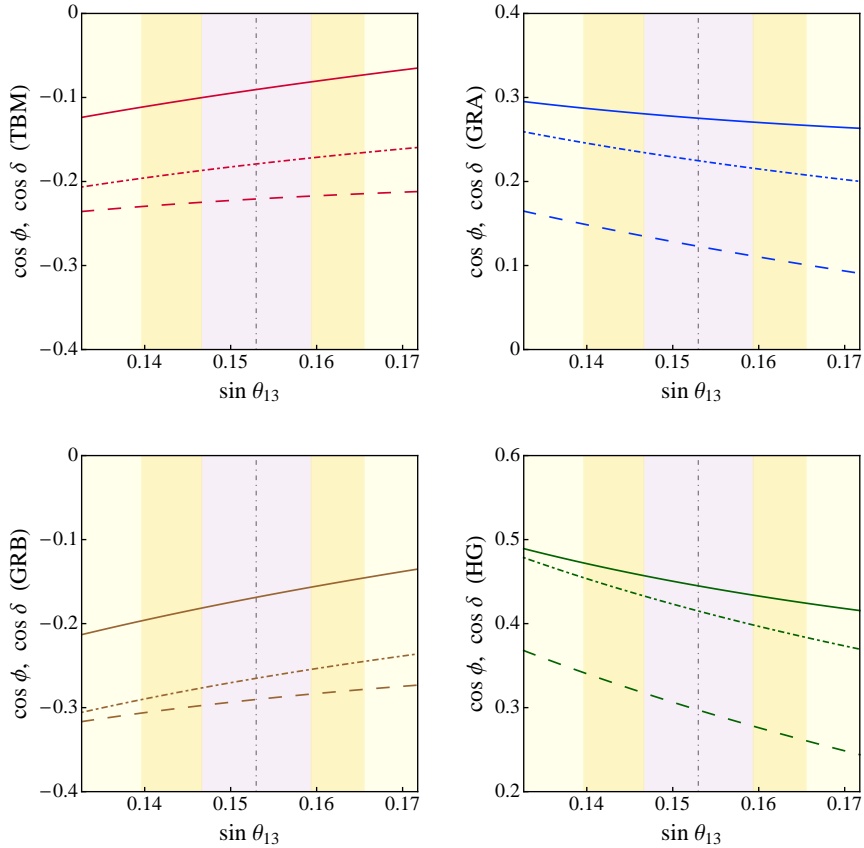


Figure 5: Predictions for $\cos \delta$ and $\cos \phi$ in the cases of TBM (upper left panel), GRA (upper right panel), GRB (lower left panel) and HG (lower right panel) forms of the matrix \tilde{U}_ν , as functions of $\sin \theta_{13}$ and for the best fit values of $\sin^2 \theta_{12} = 0.308$ and $\sin^2 \theta_{23} = 0.437$. The solid lines (dashed lines) correspond to $\cos \delta$ ($\cos \phi$) determined from the exact sum rule given in eq. (23) (eq. (24)). The dash-dotted line in each of the 4 panels represents $(\cos \delta)_{\text{LO}} = (\cos \phi)_{\text{LO}}$ obtained from the leading order sum rule in eq. (30) (eq. (33)). The vertical dash-dotted line corresponds to the best fit value of $\sin^2 \theta_{13} = 0.0234$; the three colored vertical bands indicate the 1σ , 2σ and 3σ experimentally allowed ranges of $\sin \theta_{13}$ (see text for further details).

analysed in the preceding Section, these values differ drastically (in general, both in magnitude and sign) from the exact sum rule values of $\cos \delta$ corresponding to the best fit value and the 3σ upper bound of $\sin^2 \theta_{12} = 0.308$ and 0.359 . The dependence of $(\cos \delta)_{\text{E}}$, $(\cos \delta)_{\text{LO}}$ and $(\cos \phi)_{\text{E}}$ on $\sin^2 \theta_{12}$ under discussion is shown graphically in Fig. 8.

Further, for $\sin^2 \theta_{12} = 0.259$, the ratio $(\cos \delta)_{\text{E}}/(\cos \delta)_{\text{LO}}$ in the TBM, GRA, GRB and HG cases reads, respectively, 0.744, 0.172, 0.769 and 2.32 (see Table 5). Thus, the predictions for $\cos \delta$ of the exact and the leading order sum rules differ by the factors of 5.8 and 2.3 in the GRA and HG cases. For the upper bound of the 3σ range of $\sin^2 \theta_{12} = 0.359$, the ratio $(\cos \delta)_{\text{E}}/(\cos \delta)_{\text{LO}}$ takes the values 1.2, 0.996, 1.46 and 0.969 for the TBM, GRA, GRB and HG forms of \tilde{U}_ν , respectively (see Table 6). For the GRA and HG symmetry forms, the leading order sum rule prediction for $\cos \delta$ is very close to the exact sum rule prediction, which can also be seen in Fig. 7.

$(\sin^2 \theta_{12}, \sin^2 \theta_{23}) = (0.308, 0.437)$	TBM	GRA	GRB	HG
$(\cos \delta)_E$	-0.0906	0.275	-0.169	0.445
$(\cos \delta)_{LO}$	-0.179	0.225	-0.265	0.415
$(\cos \delta)_E/(\cos \delta)_{LO}$	0.506	1.22	0.636	1.07
$(\cos \phi)_E$	-0.221	0.123	-0.29	0.297
$(\cos \delta)_E/(\cos \phi)_E$	0.41	2.24	0.581	1.5
$(\cos \phi)_E/(\cos \phi)_{LO}$	1.23	0.547	1.1	0.716

Table 4: The predicted values of $\cos \delta$ and $\cos \phi$, obtained from the exact sum rules in eqs. (23) and (24), $(\cos \delta)_E$ and $(\cos \phi)_E$, and from the leading order sum rule in eq. (30) (eq. (33)), $(\cos \delta)_{LO} = (\cos \phi)_{LO}$, using the best fit values of $\sin^2 \theta_{13} = 0.0234$, $\sin^2 \theta_{12} = 0.308$ and $\sin^2 \theta_{23} = 0.437$, for the TBM, GRA, GRB and HG forms of the matrix \tilde{U}_ν . The values of the ratios $(\cos \delta)_E/(\cos \delta)_{LO}$, $(\cos \delta)_E/(\cos \phi)_E$ and $(\cos \phi)_E/(\cos \phi)_{LO}$ are also shown.

We will investigate next the dependence of the predictions for $\cos \delta$ and $\cos \phi$ on the value of θ_{23} given the facts that i) $\sin^2 \theta_{23}$ is determined experimentally with a relatively large uncertainty, and ii) in contrast to the leading order sum rule predictions for $\cos \delta$ and $\cos \phi$, the exact sum rule predictions depend on θ_{23} . In Figs. 9 and 10 we show the dependence of predictions for $\cos \delta$ and $\cos \phi$ on $\sin \theta_{13}$ for the best fit value of $\sin^2 \theta_{12} = 0.308$ and the 3σ lower and upper bounds of $\sin^2 \theta_{23} = 0.374$ and 0.626 , respectively. For $\sin^2 \theta_{23} = 0.374$ (0.626) and the best fit values of $\sin^2 \theta_{13}$ and $\sin^2 \theta_{12}$, the exact and the leading order sum rule results $(\cos \delta)_E$, $(\cos \phi)_E$, $(\cos \delta)_{LO} = (\cos \phi)_{LO}$ and their ratios are given in Tables 7 and 8. Comparing the values of $(\cos \delta)_E$ quoted in Tables 7 and 8 with the values given in Table 4 we note that the exact sum rule predictions for $\cos \delta$ for $\sin^2 \theta_{23} = 0.374$ (lower 3σ bound) and $\sin^2 \theta_{23} = 0.437$ (best fit value) do not differ significantly in the cases of the TBM, GRA, GRB and HG forms of \tilde{U}_ν considered. However, the differences between the predictions for $\sin^2 \theta_{23} = 0.437$ and $\sin^2 \theta_{23} = 0.626$ are rather large - by factors of 2.05, 1.25, 1.77 and 1.32 in the TBM, GRA, GRB and HG cases, respectively.

In what concerns the difference between the exact and leading order sum rules predictions for $\cos \delta$, for the best fit values of $\sin^2 \theta_{13}$ and $\sin^2 \theta_{12}$, and for $\sin^2 \theta_{23} = 0.374$, the ratio $(\cos \delta)_E/(\cos \delta)_{LO} = 0.345, 1.17, 0.494$ and 0.993 for TBM, GRA, GRB and HG forms of \tilde{U}_ν . For $\sin^2 \theta_{23} = 0.626$ we have for the same ratio $(\cos \delta)_E/(\cos \delta)_{LO} = 1.04, 1.52, 1.13$ and 1.42 . Thus, for $\sin^2 \theta_{23} = 0.374$ (0.626), the leading order sum rule prediction for $\cos \delta$ is rather precise in the HG (TBM) case. For the other symmetry forms of \tilde{U}_ν the leading order sum rule prediction for $\cos \delta$ is largely incorrect. As can be seen from Figs 5 - 10 and Tables 4 - 8, we get similar results for $\cos \phi$.

In the case of the BM (LC) form of \tilde{U}_ν , physical values of $(\cos \delta)_E$, $(\cos \phi)_E$ and $(\cos \delta)_{LO}$ can be obtained for the best fit values of $\sin^2 \theta_{13}$ and $\sin^2 \theta_{23}$ if $\sin^2 \theta_{12}$ has a relatively large value. For, e.g., $\sin^2 \theta_{12} = 0.359$, $\sin^2 \theta_{13} = 0.0234$ and $\sin^2 \theta_{23} = 0.437$ we find $(\cos \delta)_E = -0.821$, $(\cos \delta)_{LO} = -0.998$, $(\cos \phi)_E = -0.837$, and $(\cos \delta)_E/(\cos \delta)_{LO} = 0.823$.

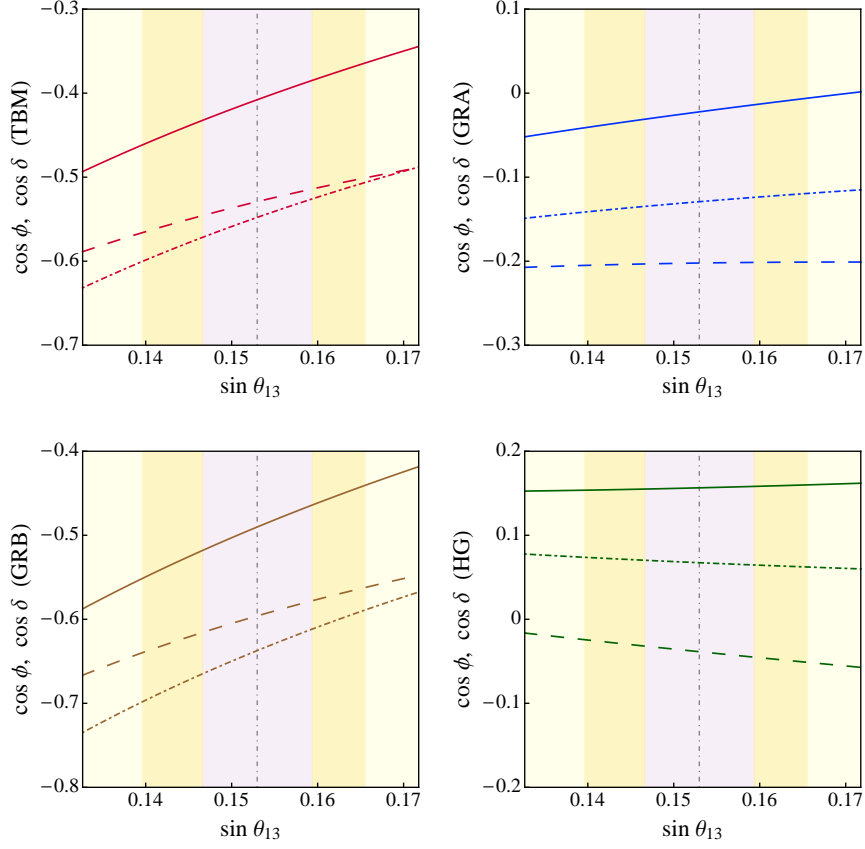


Figure 6: The same as in Fig. 5, but for $\sin^2 \theta_{12} = 0.259$ (lower bound of the 3σ interval in eq. (3)) and $\sin^2 \theta_{23} = 0.437$ (best fit value).

$(\sin^2 \theta_{12}, \sin^2 \theta_{23}) = (0.259, 0.437)$	TBM	GRA	GRB	HG
$(\cos \delta)_E$	-0.408	-0.0223	-0.49	0.156
$(\cos \delta)_{LO}$	-0.548	-0.129	-0.637	0.0673
$(\cos \delta)_E / (\cos \delta)_{LO}$	0.744	0.172	0.769	2.32
$(\cos \phi)_E$	-0.529	-0.202	-0.596	-0.0386
$(\cos \delta)_E / (\cos \phi)_E$	0.771	0.11	0.822	-4.05
$(\cos \phi)_E / (\cos \phi)_{LO}$	0.966	1.57	0.935	-0.573

Table 5: The same as in Table 4, but for $\sin^2 \theta_{13} = 0.0234$ (best fit value), $\sin^2 \theta_{12} = 0.259$ (lower bound of the 3σ range) and $\sin^2 \theta_{23} = 0.437$ (best fit value).

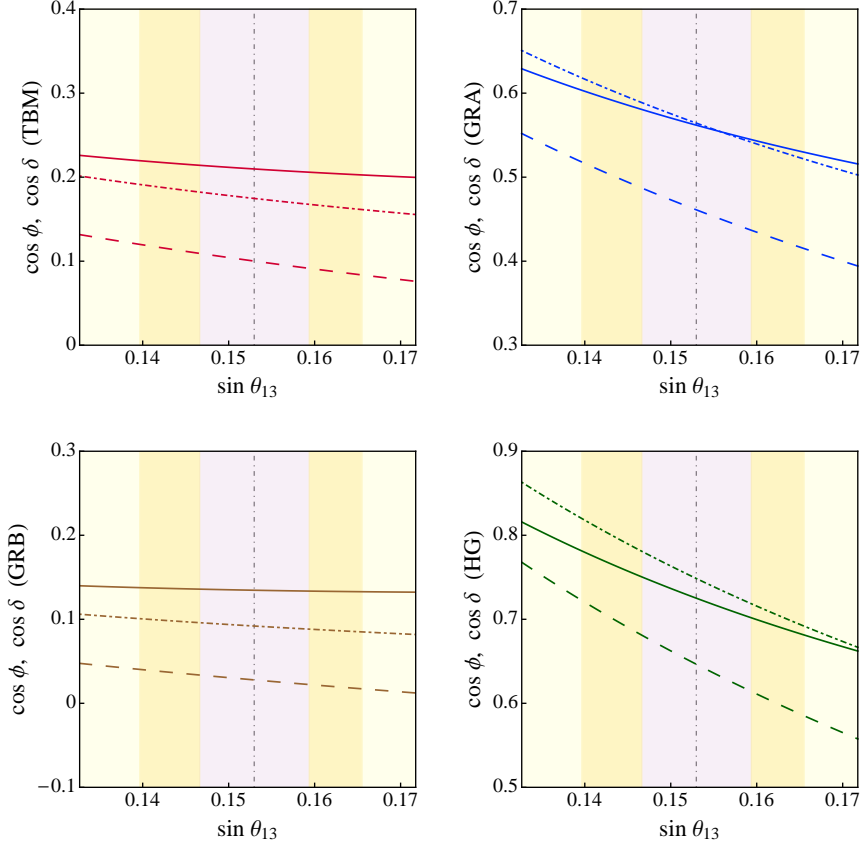


Figure 7: The same as in Fig. 5, but for $\sin^2 \theta_{12} = 0.359$ (upper bound of the 3σ interval in eq. (3)) and $\sin^2 \theta_{23} = 0.437$ (best fit value).

$(\sin^2 \theta_{12}, \sin^2 \theta_{23}) = (0.359, 0.437)$	TBM	GRA	GRB	HG
$(\cos \delta)_E$	0.21	0.562	0.135	0.725
$(\cos \delta)_{LO}$	0.175	0.564	0.092	0.749
$(\cos \delta)_E / (\cos \delta)_{LO}$	1.2	0.996	1.46	0.969
$(\cos \phi)_E$	0.1	0.461	0.0279	0.647
$(\cos \delta)_E / (\cos \phi)_E$	2.09	1.22	4.83	1.12
$(\cos \phi)_E / (\cos \phi)_{LO}$	0.573	0.817	0.303	0.864

Table 6: The same as in Table 4, but for $\sin^2 \theta_{13} = 0.0234$ (best fit value), $\sin^2 \theta_{12} = 0.359$ (upper bound of the 3σ range) and $\sin^2 \theta_{23} = 0.437$ (best fit value).

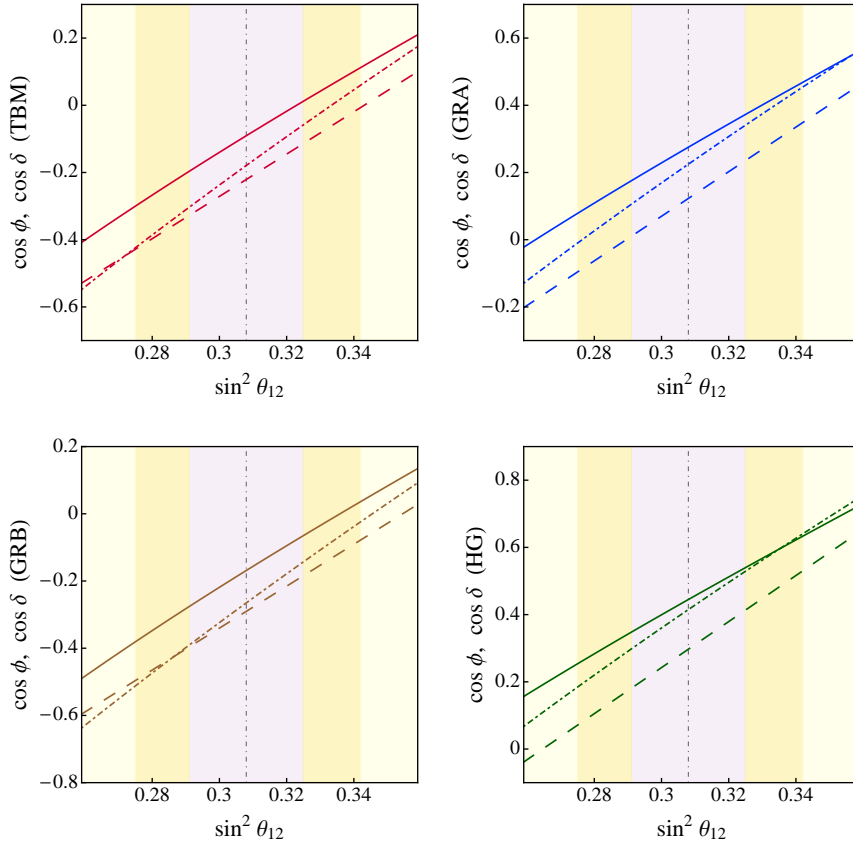


Figure 8: The same as in Fig. 5, but for $\sin^2 \theta_{13} = 0.0234$, $\sin^2 \theta_{23} = 0.437$ (best fit values) and varying $\sin^2 \theta_{12}$ in the 3σ range. The vertical dash-dotted line corresponds to the best fit value of $\sin^2 \theta_{12} = 0.308$.

Summary and Conclusions

Using the fact that the neutrino mixing matrix $U = U_e^\dagger U_\nu$, where U_e and U_ν result from the diagonalisation of the charged lepton and neutrino mass matrices, we have analysed the sum rules which the Dirac phase δ present in U satisfies when U_ν has a form dictated by flavour symmetries and U_e has a “minimal” form (in terms of angles and phases it contains) that can provide the requisite corrections to U_ν , so that the reactor, atmospheric and solar neutrino mixing angles θ_{13} , θ_{23} and θ_{12} have values compatible with the current data.

We have considered the following symmetry forms of U_ν : i) tri-bimaximal (TBM), ii) bimaximal (BM) (or corresponding to the conservation of the lepton charge $L' = L_e - L_\mu - L_\tau$ (LC)), iii) golden ratio type A (GRA), iv) golden ratio type B (GRB), and v) hexagonal (HG). For all these symmetry forms U_ν can be written as $U_\nu = \Psi_1 \tilde{U}_\nu Q_0 = \Psi_1 R_{23}(\theta_{23}^\nu) R_{12}(\theta_{12}^\nu) Q_0$, where $R_{23}(\theta_{23}^\nu)$ and $R_{12}(\theta_{12}^\nu)$ are orthogonal matrices describing rotations in the 2-3 and 1-2 planes, respectively, and Ψ_1 and Q_0 are diagonal phase matrices each containing two phases. The phases in the matrix Q_0 give contribution to the Majorana phases in the PMNS matrix.

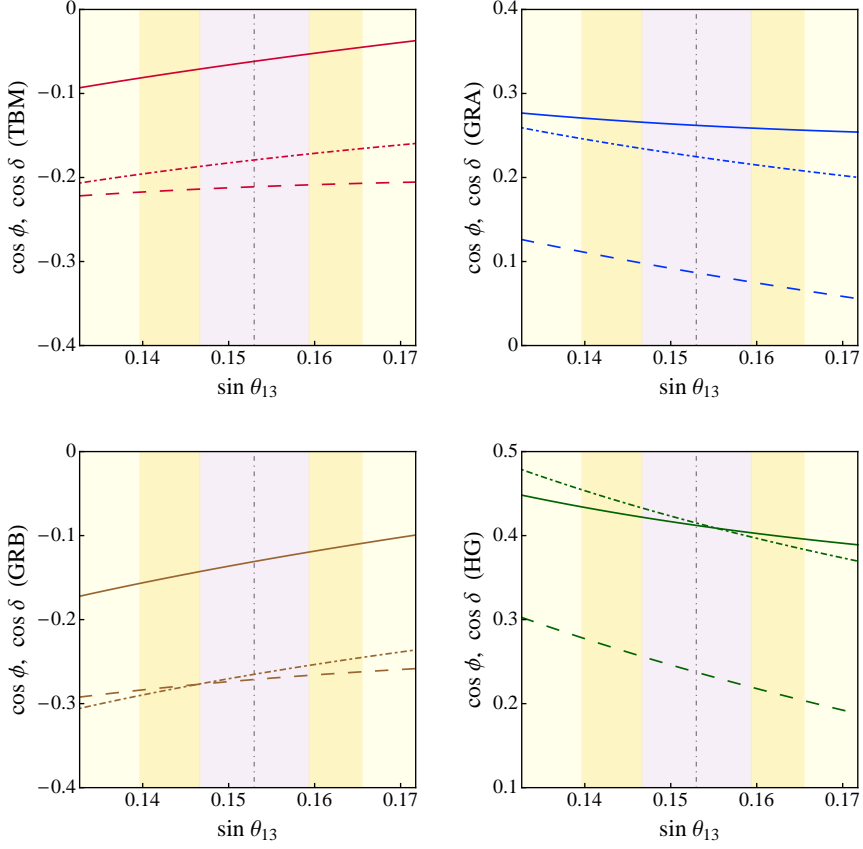


Figure 9: The same as in Fig. 5, but for $\sin^2 \theta_{12} = 0.308$ (best fit value) and $\sin^2 \theta_{23} = 0.374$ (lower bound of the 3σ interval in eq. (4)).

$(\sin^2 \theta_{12}, \sin^2 \theta_{23}) = (0.308, 0.374)$	TBM	GRA	GRB	HG
$(\cos \delta)_E$	-0.0618	0.262	-0.131	0.412
$(\cos \delta)_{LO}$	-0.179	0.225	-0.265	0.415
$(\cos \delta)_E / (\cos \delta)_{LO}$	0.345	1.17	0.494	0.993
$(\cos \phi)_E$	-0.211	0.0866	-0.271	0.237
$(\cos \delta)_E / (\cos \phi)_E$	0.293	3.03	0.483	1.74
$(\cos \phi)_E / (\cos \phi)_{LO}$	1.18	0.385	1.02	0.572

Table 7: The same as in Table 4, but for $\sin^2 \theta_{13} = 0.0234$ (best fit value), $\sin^2 \theta_{12} = 0.308$ (best fit value) and $\sin^2 \theta_{23} = 0.374$ (lower bound of the 3σ range).

The symmetry form of \tilde{U}_ν of interest, TBM, BM (LC), GRA, GRB and HG, are characterised by the same value of the angle $\theta'_{23} = -\pi/4$, but correspond to different fixed values of the angle θ'_{12} and, thus of $\sin^2 \theta'_{12}$, namely to i) $\sin^2 \theta'_{12} = 1/3$ (TBM), ii) $\sin^2 \theta'_{12} = 1/2$ (BM (LC)), iii) $\sin^2 \theta'_{12} = (2+r)^{-1} \cong 0.276$ (GRA), r being the golden ratio, $r = (1 + \sqrt{5})/2$, iv) $\sin^2 \theta'_{12} = (3-r)/4 \cong 0.345$ (GRB), and v) $\sin^2 \theta'_{12} = 1/4$ (HG).

The minimal form of U_e of interest that can provide the requisite corrections to U_ν , so

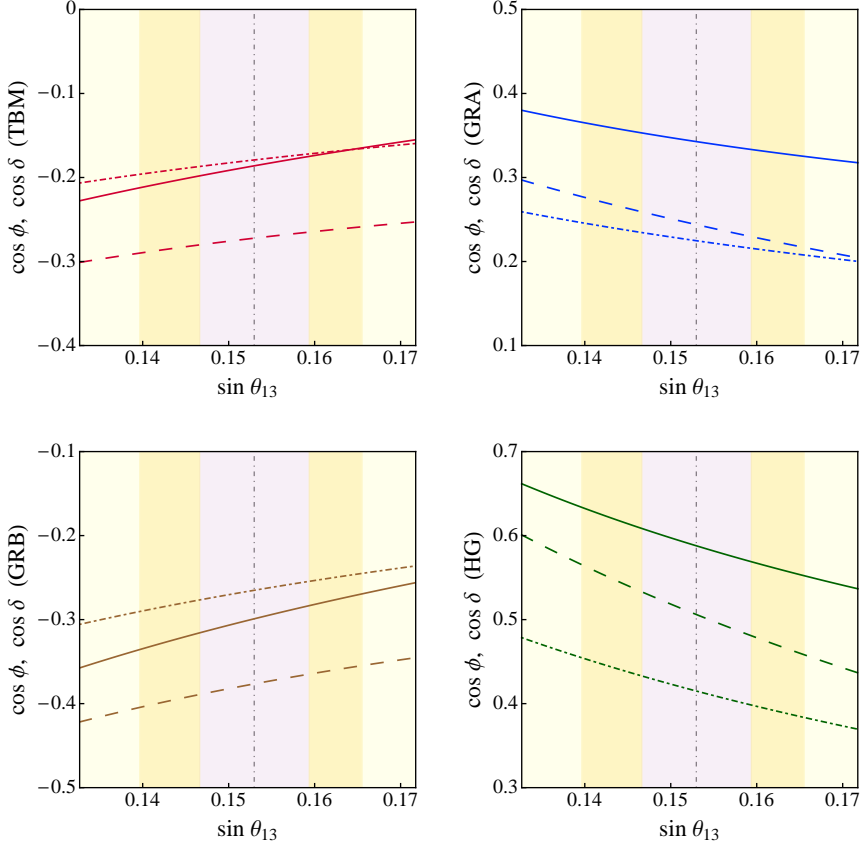


Figure 10: The same as in Fig. 5, but for $\sin^2 \theta_{12} = 0.308$ (best fit value) and $\sin^2 \theta_{23} = 0.626$ (upper bound of the 3σ interval in eq. (4)).

$(\sin^2 \theta_{12}, \sin^2 \theta_{23}) = (0.308, 0.626)$	TBM	GRA	GRB	HG
$(\cos \delta)_E$	-0.186	0.343	-0.299	0.588
$(\cos \delta)_{LO}$	-0.179	0.225	-0.265	0.415
$(\cos \delta)_E / (\cos \delta)_{LO}$	1.04	1.52	1.13	1.42
$(\cos \phi)_E$	-0.272	0.244	-0.376	0.506
$(\cos \delta)_E / (\cos \phi)_E$	0.684	1.41	0.794	1.16
$(\cos \phi)_E / (\cos \phi)_{LO}$	1.52	1.09	1.42	1.22

Table 8: The same as in Table 4, but for $\sin^2 \theta_{13} = 0.0234$ (best fit value), $\sin^2 \theta_{12} = 0.308$ (best fit value) and $\sin^2 \theta_{23} = 0.626$ (upper bound of the 3σ range).

that the neutrino mixing angles θ_{13} , θ_{23} and θ_{12} have values compatible with the current data, including a possible sizable deviation of θ_{23} from $\pi/4$, includes a product of two orthogonal matrices describing rotations in the 2-3 and 1-2 planes [13], $R_{23}(\theta_{23}^e)$ and $R_{12}(\theta_{12}^e)$, θ_{23}^e and θ_{12}^e being two (real) angles. This leads to the parametrisation of the PMNS matrix U given in eq. (11), which can be recast in the form [13]: $U = R_{12}(\theta_{12}^e)\Phi(\phi)R_{23}(\hat{\theta}_{23})R_{12}(\theta_{12}^e)\hat{Q}$, where $\Phi = \text{diag}(1, e^{i\phi}, 1)$, ϕ being a CP violation phase, $\hat{\theta}_{23}$ is a function of θ_{23}^e (see eq. (14)), and

\hat{Q} is a diagonal phase matrix. The phases in \hat{Q} give contributions to the Majorana phases in the PMNS matrix. The angle $\hat{\theta}_{23}$, however, can be expressed in terms of the angles θ_{23} and θ_{13} of the PMNS matrix (eq. (20)) and the value of $\hat{\theta}_{23}$ is fixed by the values of θ_{23} and θ_{13} .

In this scheme the four observables θ_{12} , θ_{23} , θ_{13} and the Dirac phase δ in the PMNS matrix are functions of three parameters, θ_{12}^e , $\hat{\theta}_{23}$ and ϕ . As a consequence, the Dirac phase δ can be expressed as a function of the three PMNS angles θ_{12} , θ_{23} and θ_{13} , leading to a new ‘‘sum rule’’ relating δ and θ_{12} , θ_{23} and θ_{13} . This sum rule is exact. Its explicit form depends on the symmetry form of the matrix \tilde{U}_ν , i.e., on the value of the angle θ_{12}^ν . For arbitrary fixed value of θ_{12}^ν the sum rule of interest is given in eq. (22) (or the equivalent eq. (23)) [14]. A similar exact sum rule can be derived for the phase ϕ (eq. (24)) [14].

A parametrisation of the PMNS matrix, similar to that given in eq. (11), has been effectively employed in ref. [15]. Treating $\sin \theta_{12}^e$ and $\sin \theta_{23}^e$ as small parameters, $|\sin \theta_{12}^e| \ll 1$, $|\sin \theta_{23}^e| \ll 1$, and neglecting terms of order of, or smaller than, $O((\theta_{12}^e)^2)$, $O((\theta_{23}^e)^2)$ and $O(\theta_{12}^e \theta_{23}^e)$, the following ‘‘leading order’’ sum rule was obtained in [15]: $\theta_{12} \approx \theta_{12}^\nu + \theta_{13} \cos \delta$. This sum rule, in the approximation used to obtain it, is equivalent to the sum rule $\sin \theta_{12} \approx \sin \theta_{12}^\nu + \cos \theta_{12}^\nu \sin \theta_{13} \cos \delta$, which was shown in ref. [14] to be the leading order approximation of the exact sum rule given in eq. (22) (or the equivalent eq. (23)). In the present article we have investigated the predictions for $\cos \delta$ in the cases of TBM, BM (LC), GRA, GRB and HG symmetry forms of the matrix \tilde{U}_ν using the exact and the leading order sum rules for $\cos \delta$ discussed above and given in eqs. (23) and (30). It was shown in [14], in particular, using the best fit values of the neutrino mixing parameters $\sin^2 \theta_{12}$, $\sin^2 \theta_{23}$ and $\sin^2 \theta_{13}$ and the exact sum rule results for $\cos \delta$ derived for the TBM, GRA, GRB and HG forms of \tilde{U}_ν , that the leading order sum rule provides a largely imprecise predictions for $\cos \delta$. Here we have performed a thorough study of the exact and leading order sum rule predictions for $\cos \delta$ in the TBM, BM (LC), GRA, GRB and HG cases taking into account the uncertainties in the measured values of $\sin^2 \theta_{12}$, $\sin^2 \theta_{23}$ and $\sin^2 \theta_{13}$. This allows us, in particular, to assess the accuracy of the predictions for $\cos \delta$ based on the leading order sum rules and its dependence on the values of the indicated neutrino mixing parameters when the latter are varied in their respective 3σ experimentally allowed ranges. In contrast to the leading order sum rule, the exact sum rule for $\cos \delta$ depends not only on θ_{12} and θ_{13} , but also on $\sin^2 \theta_{23}$, and we have investigated this dependence as well.

We find that the exact sum rule predictions for $\cos \delta$ vary significantly with the symmetry form of \tilde{U}_ν . For the best fit values of $\sin^2 \theta_{12} = 0.308$, $\sin^2 \theta_{13} = 0.0234$ and $\sin^2 \theta_{23} = 0.437$, for instance, we get $\cos \delta = (-0.0906)$, (-1.16) , 0.275 , (-0.169) and 0.445 for the TBM, BM (LC), GRA, GRB and HG forms, respectively. The unphysical value of $\cos \delta$ in the BM (LC) case is a reflection of the fact that the scheme under discussion with BM (LC) form of the matrix \tilde{U}_ν does not provide a good description of the current data on θ_{12} , θ_{23} and θ_{13} [13]. Physical values of $\cos \delta$ can be obtained for the best fit values of $\sin^2 \theta_{13}$ and $\sin^2 \theta_{23}$ if $\sin^2 \theta_{12}$ has a relatively large value: for, e.g., $\sin^2 \theta_{12} = 0.34$ allowed at 2σ by the current data we have $\cos \delta = -0.943$.

The results quoted above imply that the measurement of $\cos \delta$ can allow us to distinguish between the different symmetry forms of \tilde{U}_ν [14] provided $\sin^2 \theta_{12}$, $\sin^2 \theta_{13}$ and $\sin^2 \theta_{23}$ are known with a sufficiently good precision. Even determining the sign of $\cos \delta$ will be sufficient to eliminate some of the possible symmetry forms of \tilde{U}_ν .

We find also that the exact sum rule predictions for $\cos \delta$ exhibit strong dependence on the value of $\sin^2 \theta_{12}$ when the latter is varied in its 3σ experimentally allowed range ($0.259 - 0.359$) (Tables 1 - 6). The predictions for $\cos \delta$ change significantly not only in magnitude, but also

the sign of $\cos \delta$ can change. In the case of $\theta_{23}^e = 0$, for instance, we get for the TBM form of \tilde{U}_ν for the three values of $\sin^2 \theta_{12} = 0.308, 0.259$ and 0.359 : $\cos \delta = (-0.114), (-0.469)$ and 0.221 , thus $\cos \delta = 0$ is allowed for a certain value of $\sin^2 \theta_{12}$. For the GRA and GRB forms of \tilde{U}_ν we have, respectively, $\cos \delta = 0.289, (-0.044), 0.609$, and $\cos \delta = (-0.200), -0.559, 0.138$. Similarly, for the HG form we find for the three values $\sin^2 \theta_{12}$: $\cos \delta = 0.476, 0.153, 0.789$.

We have investigated the dependence of the exact sum rule predictions for $\cos \delta$ in the cases of the symmetry forms of \tilde{U}_ν considered on the value of $\sin^2 \theta_{23}$ varying the latter in the respective 3σ allowed interval $0.374 \leq \sin^2 \theta_{23} \leq 0.626$ (Figs. 9 and 10, and Tables 7 and 8). The results we get for $\sin^2 \theta_{23} = 0.374$ and $\sin^2 \theta_{23} = 0.437$, setting $\sin^2 \theta_{12}$ and $\sin^2 \theta_{13}$ to their best fit values, do not differ significantly. However, the differences between the predictions for $\cos \delta$ obtained for $\sin^2 \theta_{23} = 0.437$ and for $\sin^2 \theta_{23} = 0.626$ are rather large - they differ by the factors of 2.05, 1.25, 1.77 and 1.32 in the TBM, GRA, GRB and HG cases, respectively.

In all cases considered, having the exact sum rule results for $\cos \delta$, we could investigate the precision of the leading order sum rule predictions for $\cos \delta$. We find that the leading order sum rule predictions for $\cos \delta$ are, in general, imprecise and in many cases are largely incorrect, the only exception being the case of BM (LC) form of \tilde{U}_ν [14]. For the best fit values of $\sin^2 \theta_{12}$, $\sin^2 \theta_{23}$ and $\sin^2 \theta_{13}$, for instance, the exact sum rule predictions for $\cos \delta$ for the TBM, GRA, GRB and HG forms of \tilde{U}_ν differ by the factors 0.506, 1.22, 0.636 and 1.07, respectively, from the predictions obtained with the leading order sum rule. There are a few cases corresponding to the maximal or the minimal 3σ value of $\sin^2 \theta_{12}$ or $\sin^2 \theta_{23}$, for which the prediction of the leading order sum rule for a given symmetry form of \tilde{U}_ν is rather precise. For, e.g., $\sin^2 \theta_{12} = 0.308$, $\sin^2 \theta_{13} = 0.0234$ and $\sin^2 \theta_{23} = 0.626$ and the TBM form we get that the exact and the leading order sum rules give, respectively, (-0.186) and (-0.179) . For the GRA, GRB and HG forms, however, we find from the exact sum rule $\cos \delta = 0.343, (-0.299)$ and 0.588 , while from the leading order sum rule we obtain values which differ respectively by the factors 1.52, 1.13 and 1.42 (Table 8).

We have performed a similar analysis of the predictions for the cosine of the phase ϕ . The phase ϕ is related to, but does not coincide with, the Dirac phase δ . The parameter $\cos \phi$ obeys a leading order sum rule which is almost identical to the leading order sum rule satisfied by $\cos \delta$. This leads to the confusing identification of ϕ with δ : the exact sum rules satisfied by $\cos \phi$ and $\cos \delta$ differ significantly. Correspondingly, the predicted values of $\cos \phi$ and $\cos \delta$ in the cases of the TBM, GRA, GRB and HG symmetry forms of \tilde{U}_ν considered by us also differ significantly (see Figs. 1 - 10 and Tables 1 - 8). This conclusion is not valid for the BM (LC) form: for this form the exact sum rule predictions for $\cos \phi$ and $\cos \delta$ are rather similar. The phase ϕ appears in a large class of models of neutrino mixing and neutrino mass generation and serves as a “source” for the Dirac phase δ in these models.

In the present article we have derived predictions for the cosine of the Dirac phase δ , present in the PMNS matrix, but have not discussed the corresponding predictions for the rephasing invariant J_{CP} associated with the Dirac phase δ , which determines the magnitude of CP violation effects in neutrino oscillations [42]. Predictions for the rephasing invariant J_{CP} in the approach considered in the present article will be presented elsewhere [43].

It follows from the results obtained in the present study that the experimental measurement of the cosine of the Dirac phase δ of the PMNS neutrino mixing matrix can provide unique information about the possible discrete symmetry origin of the observed pattern of neutrino mixing.

Acknowledgements

This work was supported in part by the European Union FP7 ITN INVISIBLES (Marie Curie Actions, PITN-GA-2011-289442-INVISIBLES), by the INFN program on ‘‘Theoretical Astroparticle Physics’’ and by the World Premier International Research Center Initiative (WPI Initiative), MEXT, Japan (STP).

A Appendix

In this section we present the relations between the phases of the two different parametrisations of the PMNS matrix employed in [15] and [14]. Using the parametrization used in [15] the PMNS matrix after setting $\theta_{13}^e = \theta_{13}^\nu = 0$ reads

$$U_{\text{PMNS}} = U_{12}^{eL\dagger} U_{23}^{eL\dagger} U_{23}^{\nu L} U_{12}^{\nu L}, \quad (47)$$

where the subscripts 12 and 23 stand for the rotation plane, e.g., the matrix U_{12}^{eL} being defined as

$$U_{12}^{eL} = \begin{pmatrix} \cos \theta_{12}^e & \sin \theta_{12}^e e^{-i\delta_{12}^e} & 0 \\ -\sin \theta_{12}^e e^{i\delta_{12}^e} & \cos \theta_{12}^e & 0 \\ 0 & 0 & 1 \end{pmatrix}, \quad (48)$$

and the others analogously. We can factorise the phases in the charged lepton and the neutrino sector in the following way:

$$\begin{aligned} U_{12}^{eL\dagger} U_{23}^{eL\dagger} &= \begin{pmatrix} 1 & 0 & 0 \\ 0 & e^{i(\delta_{12}^e + \pi)} & 0 \\ 0 & 0 & e^{i(\delta_{12}^e + \delta_{23}^e)} \end{pmatrix} \begin{pmatrix} \cos \theta_{12}^e & \sin \theta_{12}^e & 0 \\ -\sin \theta_{12}^e & \cos \theta_{12}^e & 0 \\ 0 & 0 & 1 \end{pmatrix} \\ &\times \begin{pmatrix} 1 & 0 & 0 \\ 0 & \cos \theta_{23}^e & \sin \theta_{23}^e \\ 0 & -\sin \theta_{23}^e & \cos \theta_{23}^e \end{pmatrix} \begin{pmatrix} 1 & 0 & 0 \\ 0 & e^{-i(\delta_{12}^e + \pi)} & 0 \\ 0 & 0 & e^{-i(\delta_{12}^e + \delta_{23}^e)} \end{pmatrix}, \end{aligned} \quad (49)$$

$$\begin{aligned} U_{23}^{\nu L} U_{12}^{\nu L} &= \begin{pmatrix} 1 & 0 & 0 \\ 0 & e^{i\delta_{12}^\nu} & 0 \\ 0 & 0 & e^{i(\delta_{23}^\nu + \delta_{12}^\nu)} \end{pmatrix} \begin{pmatrix} 1 & 0 & 0 \\ 0 & \cos \theta_{23}^\nu & \sin \theta_{23}^\nu \\ 0 & -\sin \theta_{23}^\nu & \cos \theta_{23}^\nu \end{pmatrix} \\ &\times \begin{pmatrix} \cos \theta_{12}^\nu & \sin \theta_{12}^\nu & 0 \\ -\sin \theta_{12}^\nu & \cos \theta_{12}^\nu & 0 \\ 0 & 0 & 1 \end{pmatrix} \begin{pmatrix} 1 & 0 & 0 \\ 0 & e^{-i\delta_{12}^\nu} & 0 \\ 0 & 0 & e^{-i(\delta_{23}^\nu + \delta_{12}^\nu)} \end{pmatrix}. \end{aligned} \quad (50)$$

Combining eq. (49) and eq. (50) and comparing with the parametrisation of the PMNS matrix employed in [14] and given in eqs. (11) and (12), we find the following relations:

$$\psi = \delta_{12}^e - \delta_{12}^\nu + \pi, \quad \omega = \delta_{23}^e + \delta_{12}^e - \delta_{23}^\nu - \delta_{12}^\nu, \quad (51)$$

$$\xi_{21} = -2\delta_{12}^\nu, \quad \xi_{31} = -2(\delta_{12}^\nu + \delta_{23}^\nu). \quad (52)$$

References

- [1] K. Nakamura and S. T. Petcov, in J. Beringer *et al.* (Particle Data Group), Phys. Rev. D **86** (2012) 010001.
- [2] S. K. Agarwalla *et al.*, arXiv:1312.6520; C. Adams *et al.*, arXiv:1307.5700; A. de Gouvea *et al.*, arXiv:1310.4340.
- [3] N. Cabibbo, Phys. Lett. B **72** (1978) 333.
- [4] S. M. Bilenky, J. Hosek and S. T. Petcov, Phys. Lett. B **94** (1980) 495.
- [5] S. M. Bilenky and S. T. Petcov, Rev. Mod. Phys. **59** (1987) 671.
- [6] S. M. Bilenky, S. Pascoli and S. T. Petcov, Phys. Rev. D **64** (2001) 053010; S. T. Petcov, Physica Scripta **T121** (2005) 94.
- [7] W. Rodejohann, Int. J. Mod. Phys. E **20** (2011) 1833.
- [8] P. Langacker *et al.*, Nucl. Phys. B **282** (1987) 589.
- [9] S. Pascoli, S. T. Petcov and A. Riotto, Phys. Rev. D **75** (2007) 083511.
- [10] S. Pascoli, S. T. Petcov and A. Riotto, Nucl. Phys. B **774** (2007) 1.
- [11] F. Capozzi, G. L. Fogli, E. Lisi, A. Marrone, D. Montanino and A. Palazzo, Phys. Rev. D **89** (2014) 093018.
- [12] M. C. Gonzalez-Garcia, M. Maltoni and T. Schwetz, arXiv:1409.5439 [hep-ph].
- [13] D. Marzocca, S. T. Petcov, A. Romanino and M. C. Sevilla, JHEP **1305** (2013) 073.
- [14] S. T. Petcov, arXiv:1405.6006v2 [hep-ph].
- [15] S. Antusch and S. F. King, Phys. Lett. B **631** (2005) 42.
- [16] S. F. King, JHEP **0508** (2005) 105.
- [17] S. F. King, A. Merle, S. Morisi, Y. Shimizu and M. Tanimoto, New J. Phys. **16** (2014) 045018.
- [18] S. F. King, talk given at Neutrino Oscillation Workshop, Conca Specchiulla (Otranto, Lecce, Italy), September 7-14, 2014, <http://www.ba.infn.it/~now/now2014/web-content/index.html>.
- [19] Y. Shimizu and M. Tanimoto, arXiv:1405.1521.
- [20] P. F. Harrison, D. H. Perkins and W. G. Scott, Phys. Lett. B **530** (2002) 167; Phys. Lett. B **535** (2002) 163; Z. Z. Xing, Phys. Lett. B **533** (2002) 85; X. G. He and A. Zee, Phys. Lett. B **560** (2003) 87; see also L. Wolfenstein, Phys. Rev. D **18** (1978) 958.
- [21] S. T. Petcov, Phys. Lett. B **110** (1982) 245.

- [22] F. Vissani, [arXiv:hep-ph/9708483]; V. D. Barger, S. Pakvasa, T. J. Weiler and K. Whisnant, Phys. Lett. B **437** (1998) 107; A. J. Baltz, A. S. Goldhaber and M. Goldhaber, Phys. Rev. Lett. **81** (1998) 5730.
- [23] L. L. Everett and A. J. Stuart, Phys. Rev. D **79** (2009) 085005.
- [24] Y. Kajiyama, M. Raidal and A. Strumia, Phys. Rev. D **76** (2007) 117301.
- [25] W. Rodejohann, Phys. Lett. B **671** (2009) 267; A. Adulpravitchai, A. Blum and W. Rodejohann, New J. Phys. **11** (2009) 063026.
- [26] C. H. Albright, A. Dueck and W. Rodejohann, Eur. Phys. J. C **70** (2010) 1099. [arXiv:1004.2798 [hep-ph]].
- [27] P. H. Frampton, S. T. Petcov and W. Rodejohann, Nucl. Phys. B **687** (2004) 31.
- [28] I. Girardi *et al.*, JHEP **1402** (2014) 050.
- [29] D. Marzocca, S. T. Petcov, A. Romanino, M. Spinrath, JHEP **11** (2011) 009.
- [30] G. Altarelli, F. Feruglio and I. Masina, Nucl. Phys. B **689** (2004) 157; I. Masina, Phys. Lett. B **633** (2006) 134.
- [31] S. Antusch and V. Maurer, Phys. Rev. D **84** (2011) 117301; A. Meroni, S. T. Petcov and M. Spinrath, Phys. Rev. D **86** (2012) 113003; S. Antusch, C. Gross, V. Maurer and C. Sluka, Nucl. Phys. B **866** (2013) 255.
- [32] M. -C. Chen and K. T. Mahanthappa, Phys. Lett. B **681** (2009) 444; M. -C. Chen, J. Huang, K. T. Mahanthappa and A. M. Wijangco, JHEP **1310** (2013) 112.
- [33] W. Chao and Y. j. Zheng, JHEP **1302** (2013) 044; D. Meloni, JHEP **1202** (2012) 090; G. Altarelli, F. Feruglio, L. Merlo and E. Stamou, JHEP **1208** (2012) 021; G. Altarelli, F. Feruglio and L. Merlo, [arXiv:1205.5133]; F. Bazzocchi and L. Merlo, [arXiv:1205.5135].
- [34] C. H. Albright and M.-C. Chen, Phys. Rev. D **74** (2006) 113006.
- [35] J. Kile, M. J. Pérez, P. Ramond and J. Zhang, Phys. Rev. D **90** (2014) 013004; C. C. Li and G. J. Ding, arXiv:1408.0785 [hep-ph]; C. C. Li and G. J. Ding, arXiv:1408.0785 [hep-ph]; S. Antusch *et al.*, arXiv:1405.6962 [hep-ph].
- [36] C. Giunti and M. Tanimoto, Phys. Rev. D **66** (2002) 053013, and Phys. Rev. D **66** (2002) 113006.
- [37] A. Romanino, Phys. Rev. D **70** (2004) 013003.
- [38] L. J. Hall and G. G. Ross, JHEP **1311** (2013) 091; Z. Liu and Y. L. Wu, Phys. Lett. B **733** (2014) 226; S. K. Garg and S. Gupta, JHEP **1310** (2013) 128; S. Gollu, K. N. Deepthi and R. Mohanta, Mod. Phys. Lett. A **28** (2013) 31, 1350131.
- [39] S. F. King and C. Luhn, Rept. Prog. Phys. **76** (2013) 056201.
- [40] G. Altarelli and F. Feruglio, Rev. Mod. Phys. **82** (2010) 2701.

- [41] K. A. Hochmuth, S. T. Petcov and W. Rodejohann, Phys. Lett B **654** (2007) 177.
- [42] P. I. Krastev and S. T. Petcov, Phys. Lett. B **205** (1988) 84.
- [43] I. Girardi, S. T. Petcov and A. V. Titov, in preparation.